Negative microfilm 64–897
received from university

TROWBRIDGE, John Charles, 1934–
THERMODYNAMIC FUNCTIONS AND PHASE TRANSITIONS INCLUDING FUSION FOR PERCHLORIC ACID, PENTAERYTHRITYL FLUORIDE AND TRIETHYLENEDIAMINE.

The University of Michigan, Ph.D., 1963
Chemistry, physical

University Microfilms, Inc., Ann Arbor, Michigan

THERMODYNAMIC FUNCTIONS AND PHASE TRANSITIONS INCLUDING FUSION FOR PERCHLORIC ACID, PENTAERYTHRITYL FLUORIDE AND TRIETHYLENEDIAMINE

by

John Charles Trowbridge

A dissertation submitted in partial fulfillment
of the requirements for the degree of
Doctor of Philosophy in the
University of Michigan
1963

Doctoral Committee:

Professor Edgar F. Westrum, Jr., Chairman
Professor Lawrence O. Brockway
Instructor Dean W. Cooke
Assistant Professor John J. Eisch
Associate Professor George W. Ford

ACKNOWLEDGEMENT

The author wishes to express his gratitude especially to Professor Edgar F. Westrum, Jr. for the unlimited time, advice and patience given freely in the course of this work. He also wishes to thank Assistant Professor R.C. Taylor, Assistant Professor B. Jaselskis, and the members of the committee for their many helpful suggestions. Appreciation is also extended to Mr. Norman G. Johnston for his design innovations and machining of the thermostat and calorimeter. Cooperation and assistance were given in taking and computing the calorimetric data by Dr. B.H. Justice, H.G. Carlson, and Elfreda Chang.

The partial financial support from the United States Atomic Energy Commission in the form of research assistantships and facilities is thankfully acknowledged. In addition direct support from the Department of Chemistry in the form of three summer fellowships and a pre-Doctorate Instructorship is gratefully recognized.

TABLE OF CONTENTS

	Page
INTRODUCTION.	1
CALORIMETRIC EQUIPMENT.	5
Mark III Cryostat.	5
Calorimeter Assembly W-33.	5
Mark IV Intermediate Temperature Thermostat. . . .	10
Calorimeter Assembly W-22.	14
Measuring Circuits	20
Mark III Measuring Circuits	20
Mark IV Measuring Circuits.	25
Adiabatic Control Circuits	26
Mark III Control Circuits	26
Mark IV Control Circuits.	29
EXPERIMENTAL RESULTS.	30
Method of Calorimetric Measurements and Calculations.	30
Data and Results	32
Calibration of Intermediate Temperature Thermostat.	32
Triethylenediamine.	40
Pentaerythrityl Fluoride.	51
Perchloric Acid	63
DISCUSSION.	76
Triethylenediamine	76
Pentaerythrityl Fluoride	78
Perchloric Acid.	80
APPENDIX I	91

TABLE OF CONTENTS (Cont.)

	Page
Digital Computer Program for Vaporization and Sublimation Correction	91
BIBLIOGRAPHY.	97

LIST OF TABLES

		Page
I.	Heat Capacity of Aluminum Oxide.	33
II.	Heat Capacity of Triethylenediamine.	41
III.	Fractional Fusion of Triethylenediamine.	47
IV.	Thermodynamic Functions of Triethylenediamine. .	50
V.	Enthalpy and Entropy Increments of Triethylenediamine.	52
VI.	Heat Capacity of Pentaerythrityl Fluoride. . . .	54
VII.	Fractional Fusion of Pentaerythrityl Fluoride. .	58
VIII.	Thermodynamic Functions of Pentaerythrityl Fluoride	61
IX.	Enthalpy and Entropy Increments of Pentaerythrityl Fluoride	62
X.	Heat Capacity of Perchloric Acid	65
XI.	Fractional Fusion of Perchloric Acid	70
XII.	Thermodynamic Functions of Perchloric Acid . . .	73
XIII.	Enthalpy and Entropy Increment of Perchloric Acid	75
XIV.	Entropy of Gaseous Perchloric Acid at 298.15°K .	90
A.	Card Formats for Vaporization and Sublimation. .	94

LIST OF FIGURES

		Page
1.	Cross-Sectional Diagram of Mark II Cryostat. . . .	7
2.	Schematic Diagram of Calorimeter W-33.	9
3.	Cross-Sectional Diagram of Mark IV Intermediate Temperature Thermostat	12
4.	Schematic Diagram of Calorimeter W-22.	17
5.	Thermometer-Heater Assembly of Mark IV Thermostat.	19
6.	Closure Assembly for Calorimeter W-22.	22
7.	Photograph of Loading Assembly for Calorimeter W-22	24
8.	Schematic Diagram of Adiabatic Shield Control Circuits	28
9.	Heat Capacity of Aluminum Oxide and W-22-Heater-Thermometer-Calorimeter Assembly	35
10.	Deviation From Smooth Curve of this Research for Aluminum Oxide	37
11.	Effect of Thermal Head on Drift.	39
12.	Heat Capacity of Triethylenediamine.	45
13.	Fractional Fusion Curve for Triethylenediamine . .	49
14.	Heat Capacity of Pentaerythrityl Fluoride.	56
15.	Fractional Fusion Curve for Pentaerythrityl Fluoride	60
16.	Heat Capacity of Perchloric Acid	68
17.	Fractional Fusion Curve for Perchloric Acid. . . .	72
18.	Phase Diagram of the System Chlorine Heptoxide-Water.	82
19.	Schematic Comparison of Raman Spectra.	87
A.	Logic for Sublimation and Vaporization Correction	93

INTRODUCTION

Cryogenic calorimetric investigations have for some time been laying a firm foundation for chemical thermodynamics. "The solid state researcher is so often occasioned to acknowledge the extraordinary wealth of information that can be obtained about substances from low-temperature heat capacity determinations that one is tempted to attribute to such measurements a more fundamental significance than to any other unique method of investigation."[1] It is the intent of this research to tap this "wealth of information" for groups of substances of particular interest - especially plastically crystalline substances and perchloric acid. Bases for concern about the thermal properties of these substances will be discussed in turn.

Plastic Crystals

Timmermans[2] has noted that a number of crystalline organic substances exist which show an unusually low entropy of fusion. These compounds composed of globular molecules he has designated as forming "plastic crystals".[3] The entropy change accompanying fusion for these substances is usually less than 5 cal. $mole^{-1}$ $^{o}K.^{-1}$ in contrast to an average value of 10 to 12 cal. $mole^{-1}$ $^{o}K.^{-1}$ exhibited by most organic compounds. In such cases, at least one solid-solid transition involving a substantial entropy increment (comparable to or exceeding the magnitude of the entropy of fusion) typically

occurs such that the sum of the fusional and transitional entropies usually approximates the entropy increment of a normal organic substance. This solid-state transition may release the crystal to a state of rotational freedom similar to the liquid state by the breaking down of long range interactions.[4] This is not to imply that "free rotation" is possible but only a very rapid reorientational flip-flopping of the molecule from one preferred position to another.[5,6]

In general, crystals showing a phase evidencing plastic flow are members of high symmetry point groups. The volume evolved by the rotation of a molecule of these crystals is nearly spherical. It is reasonable that the solid phase (crystal I) stable between the transition and fusion points crystallizes in a face-centered cubic or close-packed hexagonal space group while below the transition the crystal exists in a lower symmetry. The globular nature of a plastically crystalline molecule leads to an exceptionally high melting point not exhibited by homologs which do not rotate. A relatively high triple point pressure for the crystal I phase accompanies the high melting point and, therefore, a very narrow liquid range is usually observed.

This research is concerned with the thermal behavior of two plastic crystals as studied by precise calorimetry. The fusional properties of pentaerythrityl fluoride and triethylenediamine as well as the solid state transformation to the plastically crystalline phase of the latter are studied. Such thermodynamic data characterize phase transformations in

a quantitative way and provide a sensitive tool for use in both formulating and testing theoretical interpretations of transformational processes.[7]

Perchloric Acid

A method for the preparation of perchloric acid has been known since 1818.[8] Since that time the anhydrous acid and many of its salts have been extensively investigated.[9] Uses of the aqueous acid have been limited primarily to analytical and electrolytical chemistry with little present use available for the anhydrous materials due to its instability. This instability may be related to its occurence in the asymmetrical, covalent form with little ionization taking place until dilution to 77 percent by weight with water.[10] Although the exact decomposition products of perchloric acid vary from one investigation to another,[11,12] the only apparently safe means of storage is at liquid nitrogen temperatures.[13]

Several investigators[14,15,16,17] have studied the physical properties of anhydrous perchloric acid but very little thermal data are available.[18] Five stable hydrates of the acid are known,[19,20] while enthalpies of formation have been measured for the mono-and dihydrate.[21]

Interest in the research endeavor evolved from consideration of the transition in perchloric acid monohydrate. The monohydrate exists entirely as the hydronium salt[15] ($H_3O^+ClO_4^-$) in the solid with rotation of the hydronium ion above $-25^{\circ}C$.[22] This research is the first contribution to a study of this

rotational phenomena and the perchloric acid-water system utilizing calorimetric methods. It is hoped that all the stable hydrates of perchloric acid may be studied thus providing a more complete picture of these interesting but dangerous materials.

CALORIMETRIC EQUIPMENT

Mark III Cryostat

For the adiabatic measurements of heat capacities over the range 5 to 350°K. the Mark III cryostat was employed. This cryostat, described by Carlson,[23] is similar in most features to one reported earlier by Westrum, Hatcher, and Osborne.[24] Figure 1 shows the schematic cross-section of Mark II which differs from Mark III mainly in that the latter has no economizer.

Calorimeter Assembly W-33

For the study of perchloric acid at low temperatures it was found that the conventional type of calorimeter used by this laboratory was not satisfactory. The tremendous oxidizing power of the sample made it virtually impossible to place the compound in intimate contact with metals readily used for calorimeter construction. Silver, nickel, copper, and gold specimens subjected to the anhydrous acid were readily oxidized as shown by a loss in weight and chemical tests. Platinum was tested and showed no loss in weight but did cause decomposition of the acid. Therefore, a gold-plated, copper calorimeter (laboratory designation W-33 and shown in Figure 2) was fabricated weighing 44.3 g. which accepts a glass liner, E. This liner has an internal volume of about 45 cc., weighs 36.5 g. and is surrounded by a cylindrical shell, F, 5.3 cm. long, 4.4 cm. in diameter, with walls 0.2 mm. thick. The Monel

CALORIMETRIC EQUIPMENT

Mark III Cryostat

For the adiabatic measurements of heat capacities over the range 5 to 350°K. the Mark III cryostat was employed. This cryostat, described by Carlson,[23] is similar in most features to one reported earlier by Westrum, Hatcher, and Osborne.[24] Figure 1 shows the schematic cross-section of Mark II which differs from Mark III mainly in that the latter has no economizer.

Calorimeter Assembly W-33

For the study of perchloric acid at low temperatures it was found that the conventional type of calorimeter used by this laboratory was not satisfactory. The tremendous oxidizing power of the sample made it virtually impossible to place the compound in intimate contact with metals readily used for calorimeter construction. Silver, nickel, copper, and gold specimens subjected to the anhydrous acid were readily oxidized as shown by a loss in weight and chemical tests. Platinum was tested and showed no loss in weight but did cause decomposition of the acid. Therefore, a gold-plated, copper calorimeter (laboratory designation W-33 and shown in Figure 2) was fabricated weighing 44.3 g. which accepts a glass liner, E. This liner has an internal volume of about 45 cc., weighs 36.5 g. and is surrounded by a cylindrical shell, F, 5.3 cm. long, 4.4 cm. in diameter, with walls 0.2 mm. thick. The Monel

Figure 1

Cross-Sectional Diagram of Mark II Cryostat

Legend:

1. Nitrogen inlet and outlet connector
2. Nitrogen filling tube
3. Sleeve fitting to helium transport dewar
4. Helium transfer tube
5. Screw fitting at inlet of helium transfer tube
6. Plug or extension to helium transfer tube
7. Brass vacuum can
8. Outer "floating" radiation shield
9. Nitrogen tank
10. Helium tank
11. Nitrogen radiation shield
12. Lead wire bundle
13. Helium radiation shield
14. Adiabatic shield
15. Windlass
16. Helium exit connector
17. Thermal shield for lead connectors
18. Helium exit tube
19. Vacuum seal and terminal plate for leads
20. O - ring gasket
21. Head plate
22. Coil spring
23. "Economizer"
24. Calorimeter supporting string
25. "Floating" ring
26. Calorimeter assembly

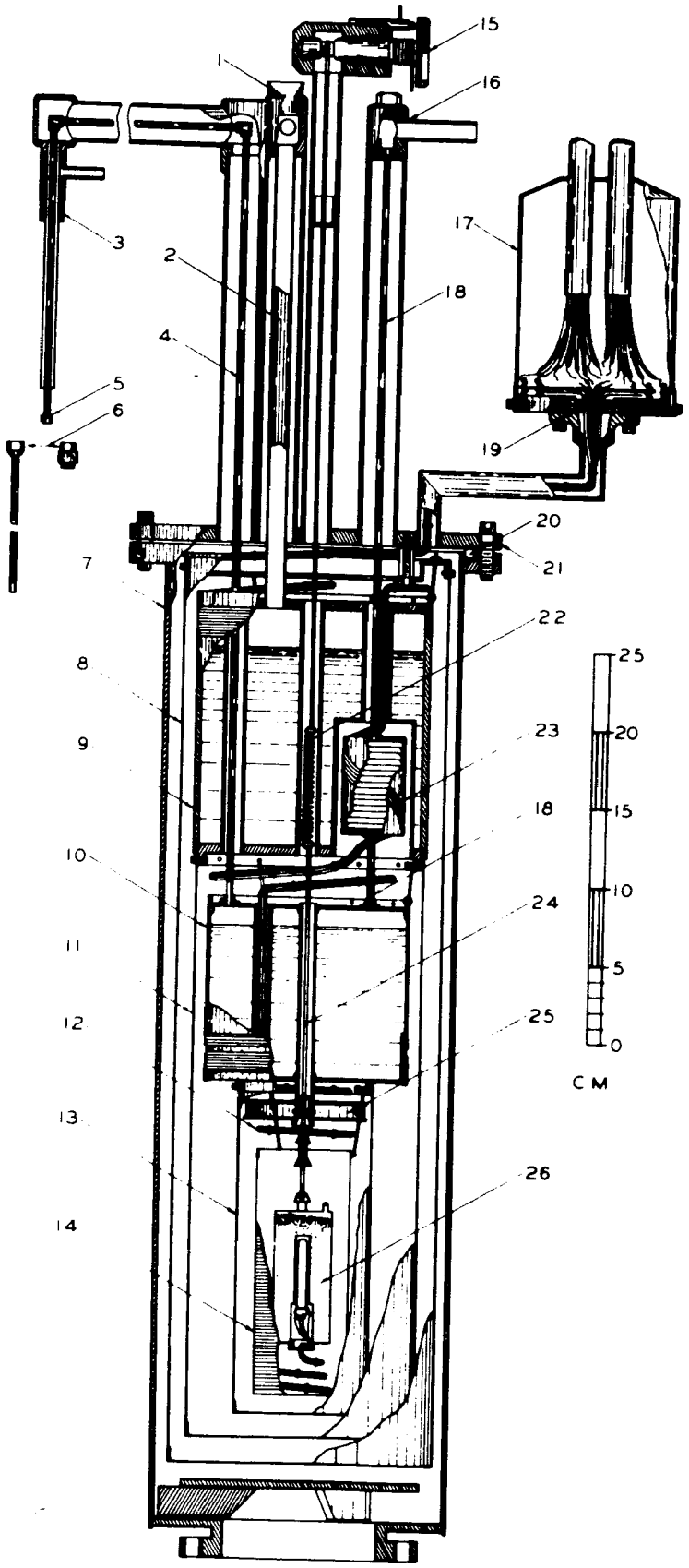

15
1
16
3
2
17
18
4
5
6
19
20
21
7
22
8
25
9
23
20
18
15
10
24
10
11
5
12
25
0
CM
13
26
14

Figure 1

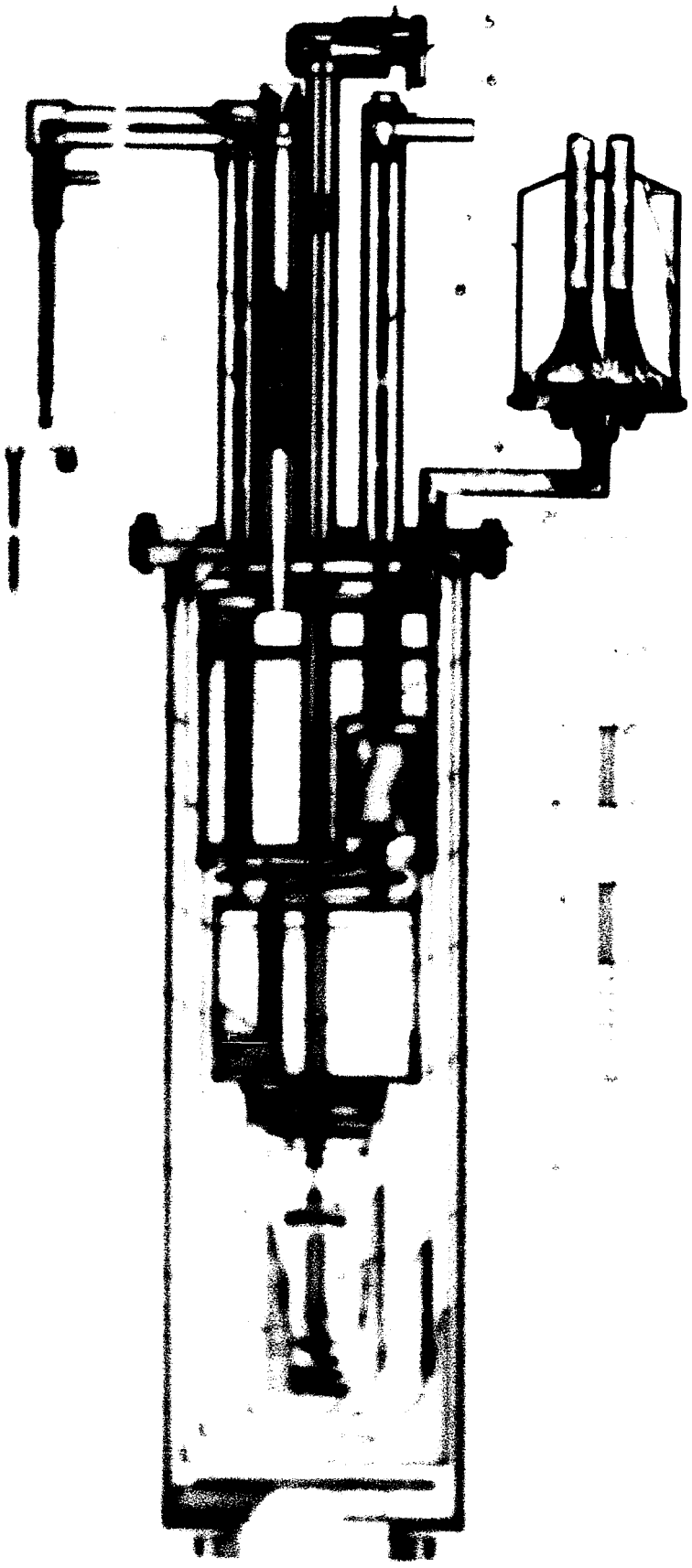


Figure 2

Schematic Diagram of Calorimeter W-33

Legend:

A. Liner filling tube

B. Thermal conductivity cone

C. Helium filling tube

D. Heater-thermometer well assembly

E. Glass liner

F. Calorimeter shell

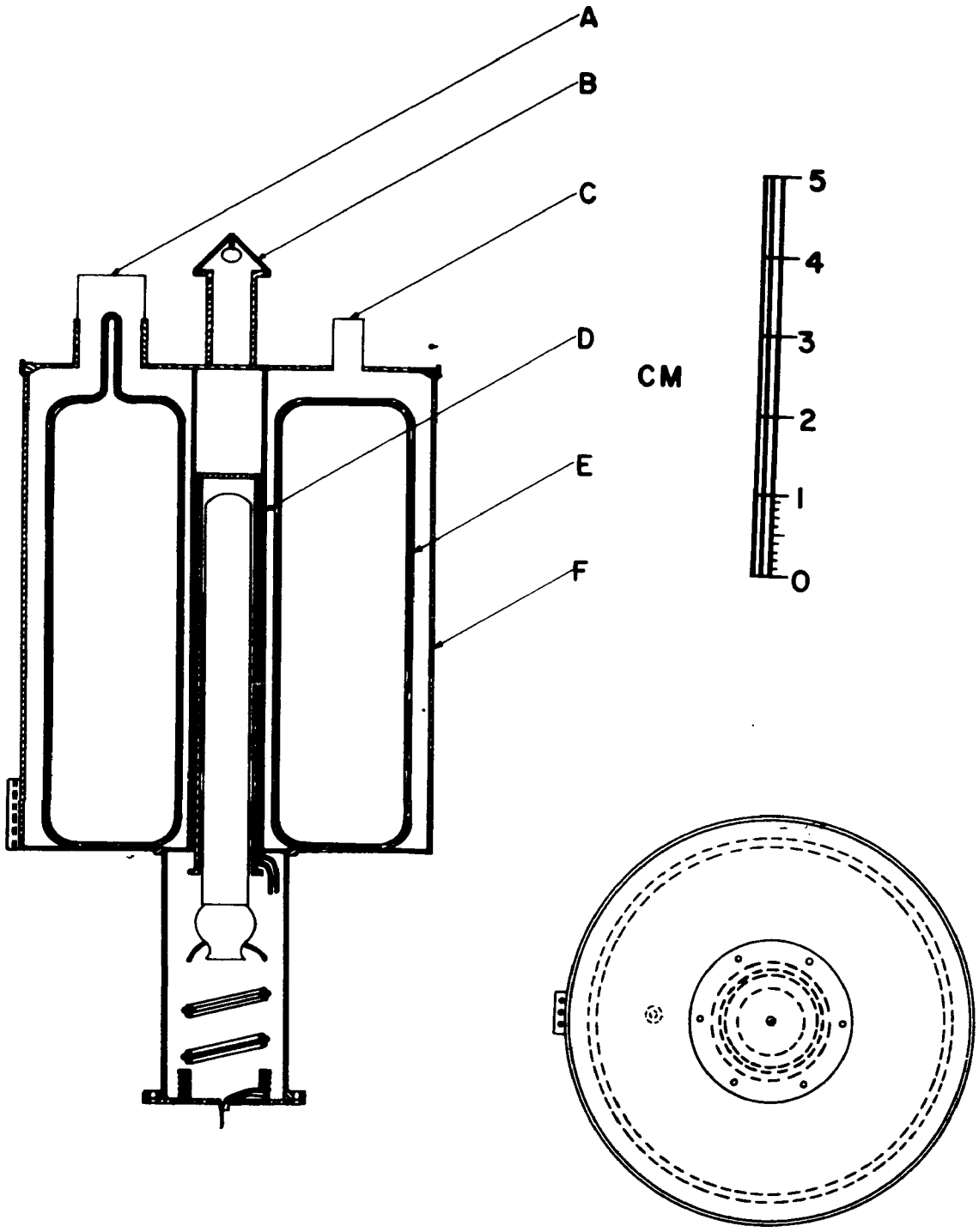


Figure 2

neck, A, allows sealing-off the filling tube of the liner after loading of the sample while a small aperture in the Monel tube, C, is sealed after helium is added for thermal contact between the glass container and calorimeter. The axial entrant well, D, accommodates the heater-thermometer assembly. The temperature sensing element is a Leeds and Northrup capsule-type, platinum-resistance thermometer within a cylindrical, copper heater sleeve wound bifilarly with Fiberglas-insulated Advance wire having a resistance of 150 ohms. Apiezon-T grease is used to provide thermal contact between thermometer, heater and calorimeter.

Mark IV Thermostat

The thermostat used in making adiabatic measurements of heat capacities in the range 250 to 600°K. is essentially a modification of the low temperature cryostats used in this laboratory. Figure 3 shows the main features of the thermostat-calorimeter unit in schematic cross-section. The high vacuum casing used with Mark IV is nearly identical with that shown earlier for Mark II; except for the nitrogen tank filling tube, the external fixtures on the top plate have been eliminated.

The large stainless steel tube shown at the top of Figure 3 is 1.91 cm. in diameter, 0.25 mm. thick and serves to support the entire thermostat-calorimeter unit within an evacuated brass can (not shown). This tube is thermally isolated from the outer top plate as is a floating radiation shield

Figure 3

Cross-Sectional Diagram of Mark IV Thermostat

Legend:

A. Guard shield ring

B. Calorimeter suspension collar

C. Primary radiation shield

D. Calorimeter closure assembly

E. Guard shield

F. Calorimeter assembly

G. Thermometer- heater assembly

H. Thermometer

I. Thermal equilibration spool

J. Lead bundle

K. Adiabatic shield

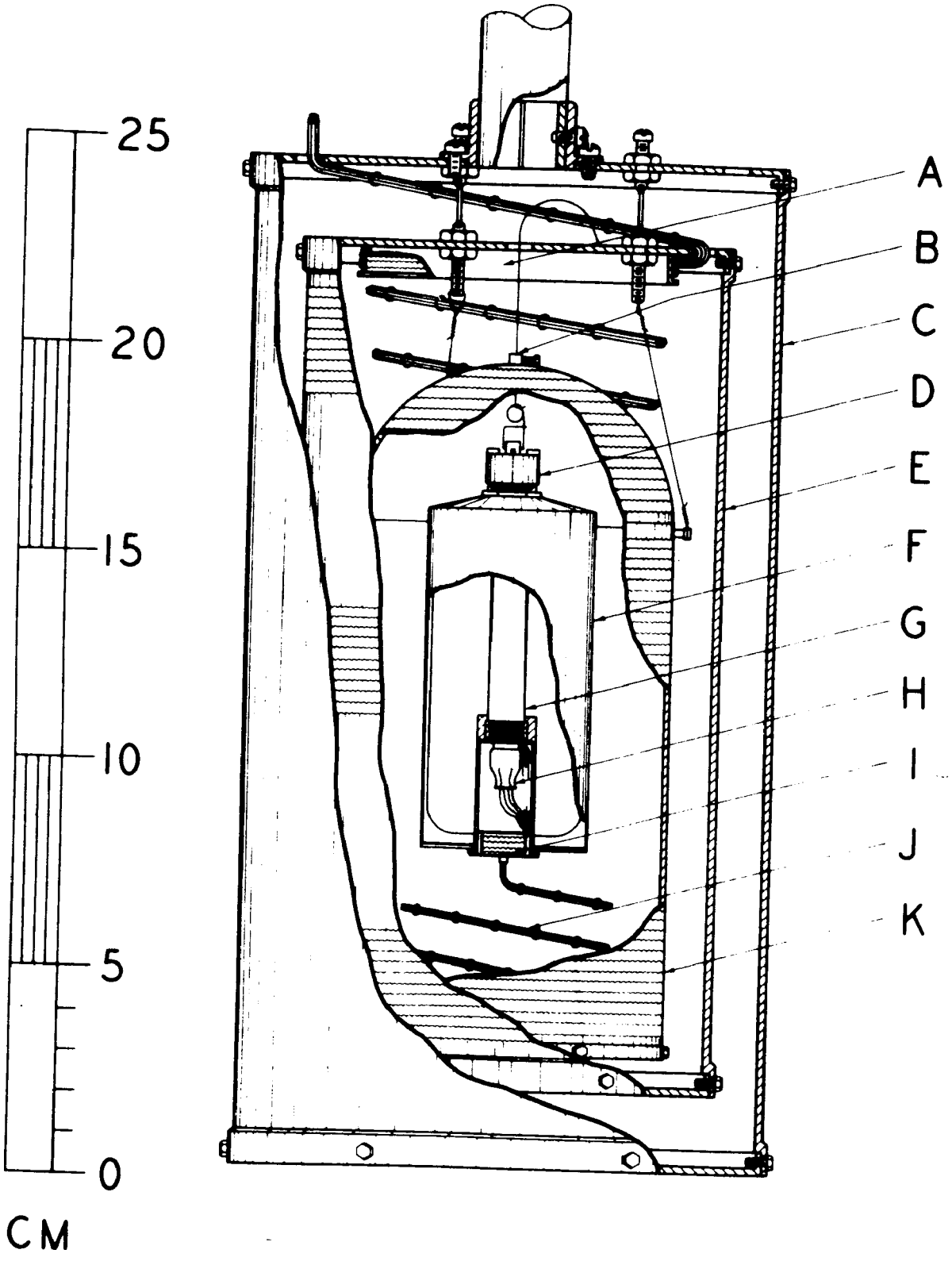


Figure 3

(not shown). This radiation shield significantly reduces the electrical power required to maintain the highest temperatures, for in contrast to most calorimeters made for operation in this range no "external furnace" is provided. The top of the primary radiation shield, C, is secured to the lower end of the large stainless steel tube. Situated between this radiation shield and the top plate is a tank of 1.5 liters capacity for liquid nitrogen coolant. A filling tube 1.25 cm. dia. thin-wall stainless steel is led through the top plate to the tank while a 4 mm. stainless steel tube provides thermal contact between the tank and the thermostat itself. In this manner the whole thermostat and calorimeter are cooled by admitting less than 0.1 mm. pressure helium gas into the vacuum chamber to provide a heat-transfer mechanism.

The guard shield, E, is supported by three machine screws (turned to a small diameter over most of their length) from the primary radiation shield and functions as the main buffer between the adiabatic shield, K, and ambient room temperature. Temperature control of this shield is maintained by two independent heaters, each about 500 ohms. The bulk of the heating is done through manually preset variable auto transformers and step resistors. Actual temperature regulation is maintained by an automatic channel, described later, set to control one to two degrees below the temperature of the calorimeter. The top and bottom of this shield are also heated by the automatic control, thereby giving a thermal atmosphere very close to that of the adiabatic shield. On

the inside of the top of the guard shield is a ring, A, a tie-down junction for the lead bundle, J, just as it arrives at a warm point. This ring allows tempering of the temperature of the leads prior to their arrival at the adiabatic shield. A copper-Constantan differential thermocouple buried in the enamelled-down bundle on the top plate of the guard shield serves as the control point for the shield. Since this shield weighs about 1.3 kilograms, it provides a very stable thermal reservoir.

The adiabatic shield, K, spun from 1.27 mm. copper, has a hemispherical top and cylindrical middle section. The open lower end of the shield is closed with a closely-fitting copper plate held in place by six hex head machine screws. Loading and unloading are readily achieved by removing the flat bottom disc. The entire surface of the top-middle section of the shield is covered with a 300 ohm Fiberglas-covered, resistance wire heater. The bottom section is covered with 500 ohms of wire. Both sections of the adiabatic shield are separately controlled automatically as in Mark III using a copper-Constantan differential thermocouple to provide the sensing potential. The top-middle section responds to a difference in temperature between the calorimeter, F, and the shield. The bottom section and the whole guard shield have the reference terminal of the differential thermocouple on the top-middle section.

Calorimeter Assembly W-22

A representation of the calorimeter used in Mark IV for

high temperature studies is shown in Figure 4. This calorimeter is similar in size and shape to those used in low temperature work but with two marked deviations in the method of sealing the top and of installing the thermometer-heater assembly. Except for the sealing mechanism the calorimeter was machined from two portions of fine silver rod. The bottom, entrant well, and six vertical, radial vanes (which provide thermal conductivity and are tapered radially to economize mass) were fabricated from one rod. The body and integral conical top portion of the calorimeter is a cylinder 3.9 cm. dia. and 0.5 mm. thick. All seams for the completed assembly were force-fitted and sealed vacuum tight by silver alloy brazing using APW #355 alloy. The calorimeter has an internal volume of 82 cc. and weighs 115 grams.

The axial entrant well is so constructed as to accept the thermometer-heater assembly shown in Figure 5. A Leeds and Northrup capsule-type, platinum-resistance thermometer is gripped in a slender beryllium copper collet arrangement. This collet in turn is screwed into the tapered heater sleeve placing the thermometer in contact with the heater sleeve via the beryllium copper. The heater contains 250 ohms of B and S #38 Karma wire wound bifilarly. A recessed groove of the heater sleeve is used to tie down the heater leads before they enter small holes under the threads and out to the calorimeter spool. It is believed that fairly good thermal contact is achieved between thermometer, heater, sample and calorimeter since equilibrium is usually achieved within thirty

Figure 4

Schematic Diagram of Calorimeter W-22

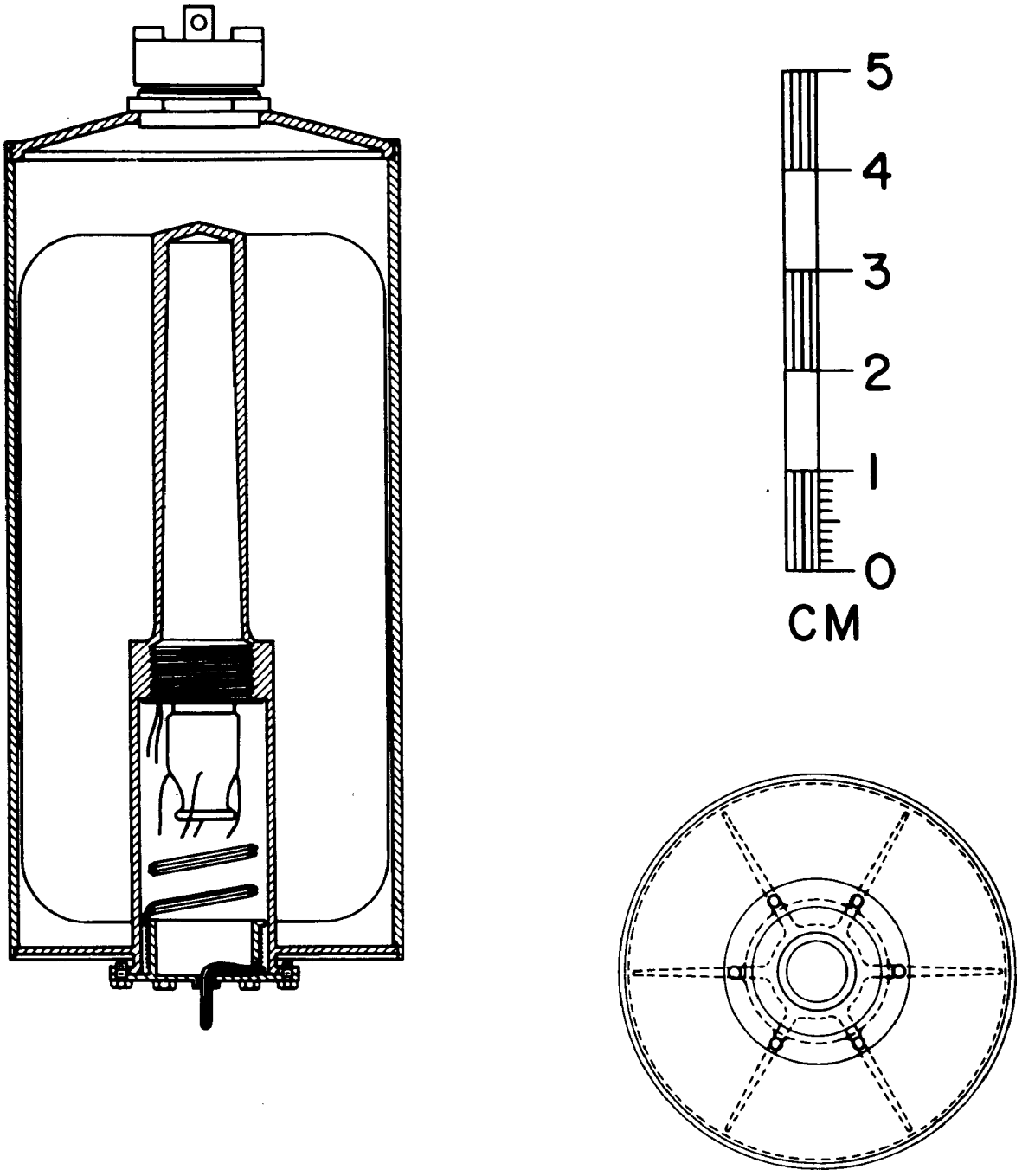


Figure 4

Figure 5

Thermometer-Heater Assembly of

Mark IV Thermostat

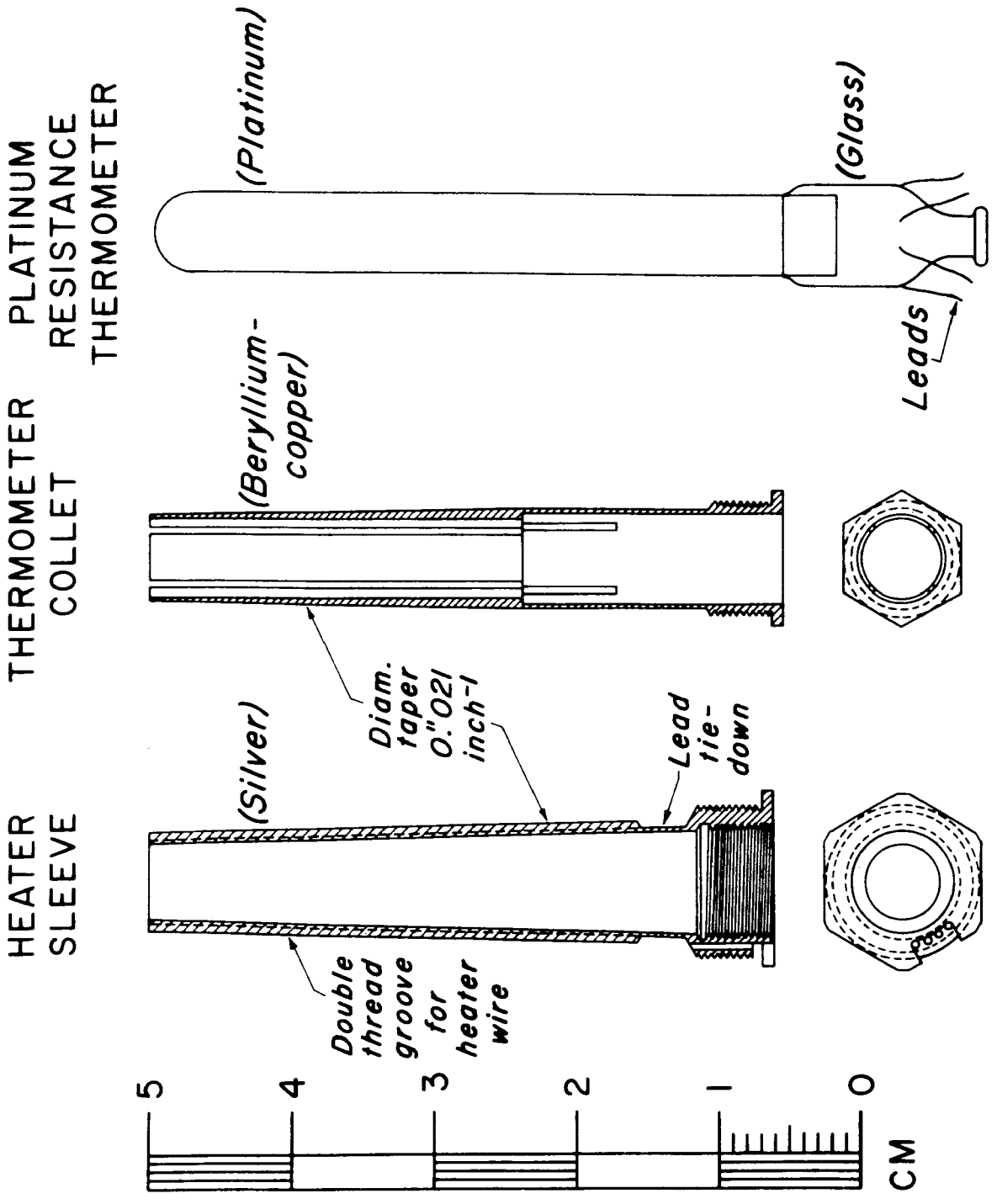

HEATER SLEEVE
THERMOMETER COLLET
PLATINUM RESISTANCE THERMOMETER
(Silver)
(Beryllium-copper)
(Platinum)
(Glass)
Diam. taper 0.002/ inch-1
Lead tie-down
Double thread groove for heater wire
Leads
5
4
3
2
1
0
CM

Figure 5

minutes after an energy input.

Figure 6 shows the closure used to eliminate a soldered seal requiring temperatures in excess of 300°C. for operation. The vacuum-tight closure is achieved by forcing the annealed gold gasket against a circular knife edge. Gasket and plate are prevented from turning during closure, thus assuring a clean cut into the gold. The inlet aperture is 1 cm. dia. and constructed of stainless steel so as to avoid locking of the threads with the Monel cap. Figure 7 shows a photograph of the calorimeter within a glass cylinder which serves as a loading assembly. The lugs on the cap fit into recesses of the externally operated, manual wrench arrangement. The glass chamber can be evacuated to 10^{-6} mm., and helium gas for thermal conduction within the sample space can then be admitted before seal-off.

Measuring Circuits

Mark III Measuring Circuits: The measurement of temperature is achieved by observing the potential drop across both the platinum-resistance thermometer and a standard resistor in series with it to yield the thermometer current. For these measurements an autocalibrated White double potentiometer is employed using one bank of dials to measure the voltage drop across the standard resistor and the other across the thermometer. To observe the degree of imbalance of the potentiometer a Leeds and Northrup Type HS galvanometer mounted on a Julius suspension is used. This galvanometer employs a 5-meter path length from telescope to scale allow-

Figure 6

Closure Assembly For Calorimeter W-22

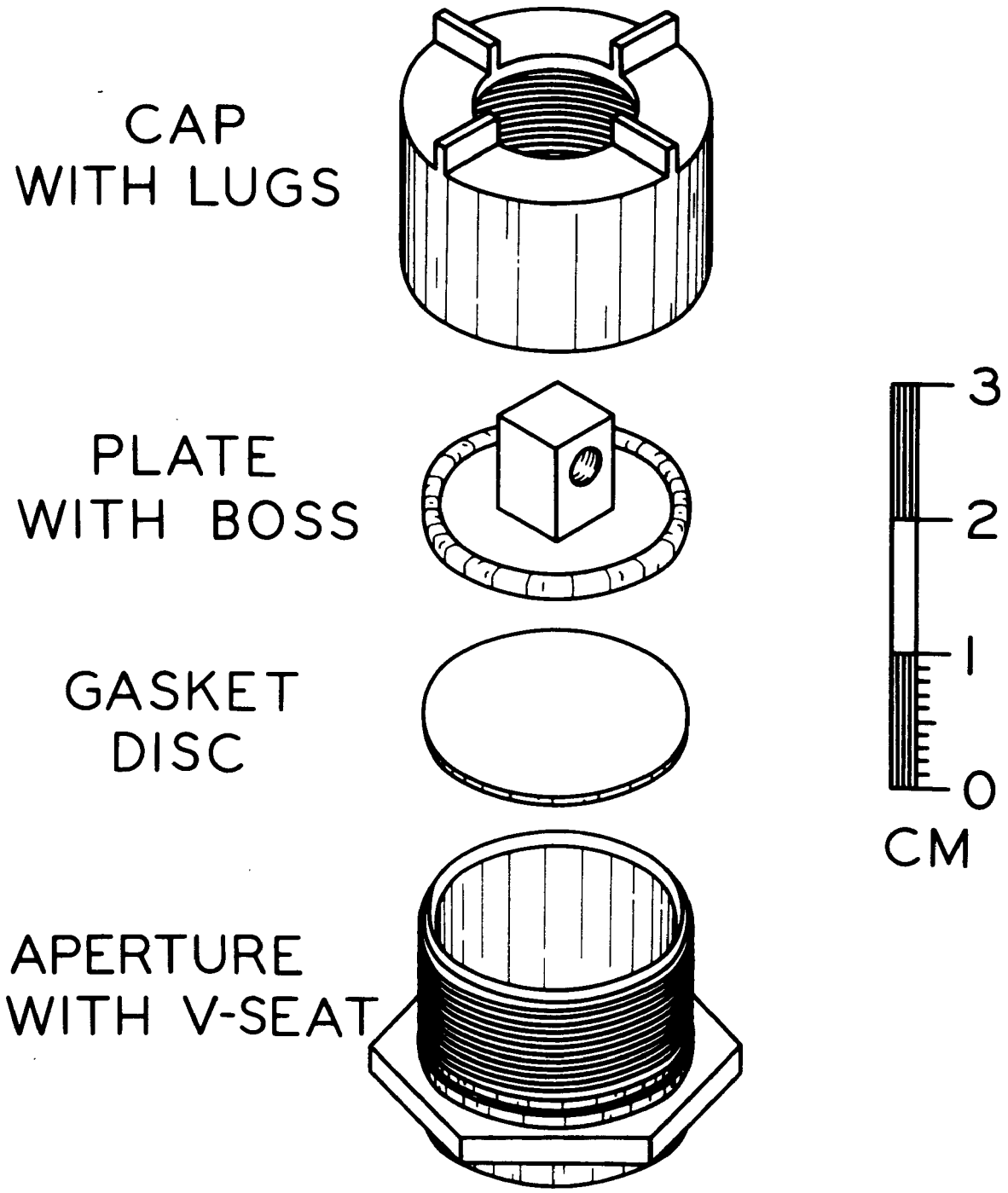

CAP
WITH LUGS
PLATE
WITH BOSS
GASKET
DISC
APERTURE
WITH V-SEAT
3
2
1
0
CM

Figure 6

Figure 7

Photograph of Loading Assembly For

Calorimeter W-22

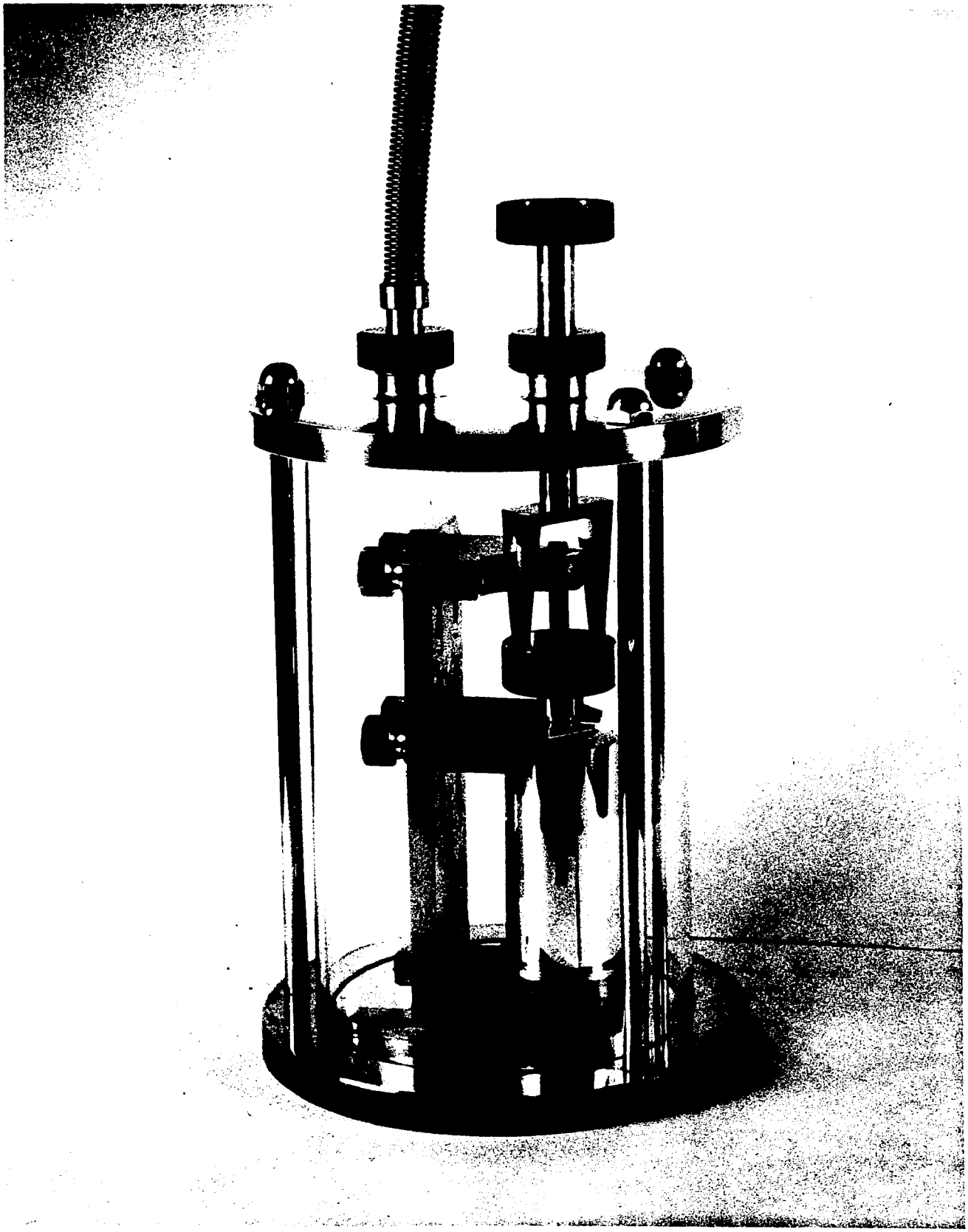


Fig. 7

ing a working sensitivity of 0.03 μv/mm. A thermometer current of 2 ma. is used above 70°K., while below this temperature 4 ma. is needed to insure high accuracy.

Potentials corresponding to the current and e.m.f. supplied to the heater as well as the potentials of the absolute thermocouples are also measured with the galvanometer-potentiometer system described above. For the duration of energy input an interval timer, powered by a precision tuning fork, is utilized to give durations from two to six minutes accurate to within 0.01 seconds. The energy is supplied by a bank of low discharge lead storage batteries arranged to give a continuously variable current from 0.7 to 210 ma. All standard resistors for voltage drop measurements and unsaturated Weston standard cells have been calibrated by the National Bureau of Standards.

Mark IV Measuring Circuits: The methods used in measuring the temperature and energy are in principle the same as described above. The potentials, however, are measured with a Rubicon double, six-dial, thermo-free potentiometer allowing direct reading either to 0.1 μv on the lower sensitivity or to 0.01 μv on the high sensitivity. The imbalance of the potentiometer is amplified through a Rubicon photo-electric galvanometer and displayed on a center reading lamp and scale galvanometer with sufficient gain to allow interpolation to 0.01 μv.

Adiabatic Control Circuits

Mark III Control Circuits: While Mark III is designed to be operated with automatic shield control, manual shield control is often used up to 70°K. Two-junction differential thermopiles are provided to facilitate the adiabatic control and are arranged to sense the temperature difference between the calorimeter-middle, middle-top, and middle-bottom of the shield. The floating ring is followed by a differential thermocouple between the middle section of the adiabatic shield and the ring. The potentials produced by the differential units are displayed on two high-sensitivity galvanometers having a working sensitivity of 0.01 μv/mm. This arrangement allows adiabatic conditions to be maintained to within 0.002°K. except for a few seconds at the start and finish of an energy input. The adiabatic heaters and the ring are powered by alternating current through circuits allowing any heater current up to 15 ma. on each of the heaters.

Completely automatic controls to maintain adiabatic conditions are useful to allow one operator to make all measurements and to provide continuous control over a period of several days while studying equilibrium transition phenomena. The controls incorporated in this laboratory are shown schematically in Figure 8 and consist of a stabilized d.c. microvolt amplifier to amplify the output from the differential thermocouple (or thermopile). The amplifier output is displayed on a Speedomax G microvolt recorder where the degree of imbalance from a preset control point is sensed and com-

Figure 8

Schematic Diagram of Adiabatic
Shield Control Circuits

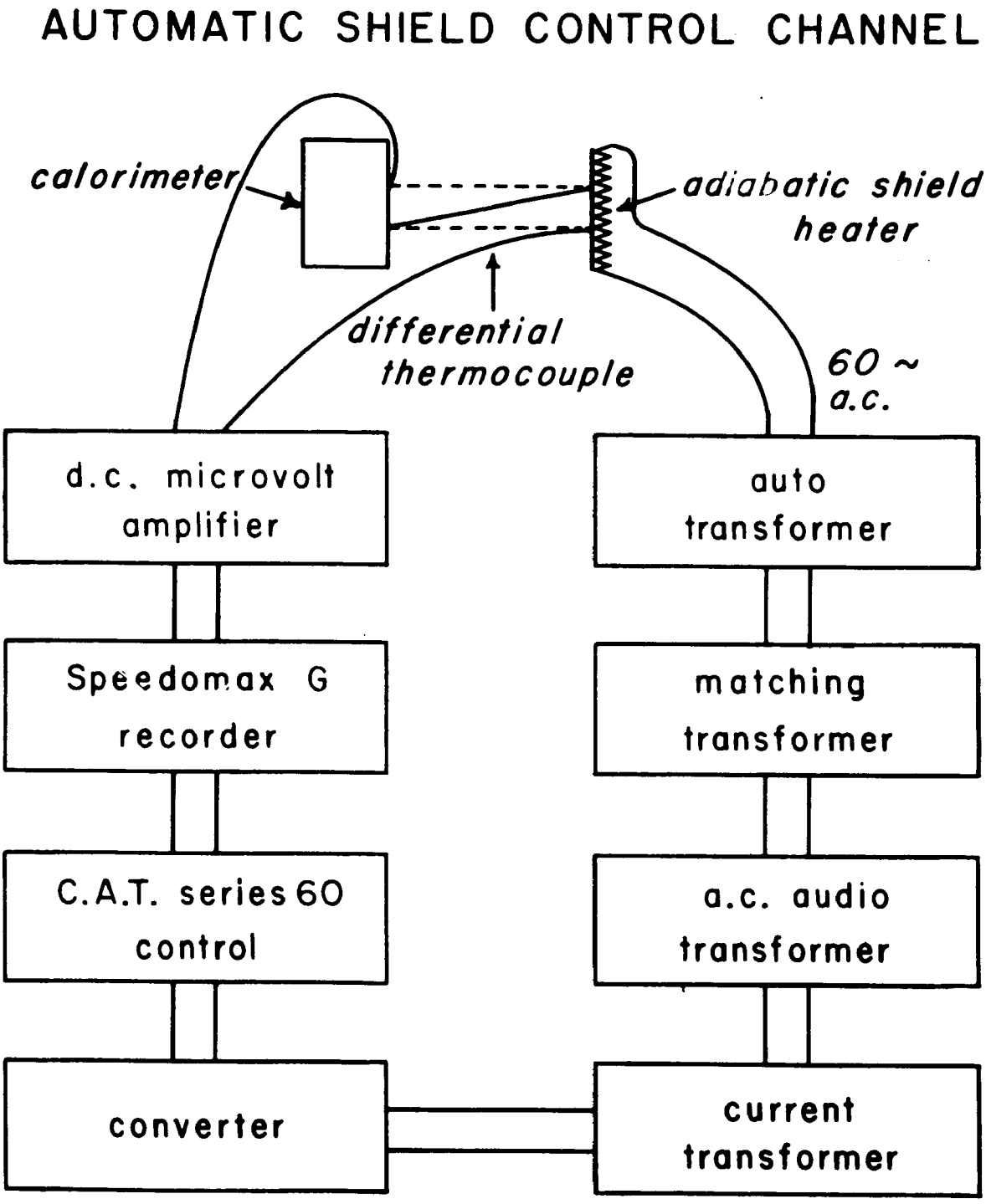

AUTOMATIC SHIELD CONTROL CHANNEL
calorimeter
adiabatic shield heater
differential thermocouple
60 ~ a.c.
d.c. microvolt amplifier
auto transformer
Speedomax G recorder
matching transformer
C.A.T. series 60 control
a.c. audio transformer
converter
current transformer

Figure 8

pensated with a Series 60 Current Adjusting Type (CAT) control system. The d.c. CAT output is converted to a.c. for amplification, and after inductance matching, is fed directly to the heater. Each of the three adiabatic heaters has its own control channel and is regulated independently. The ring heater is readily controlled manually by the potentiometer operator. In operation the automatic shield control can maintain the shields within 0.002°K. of the preset temperature. This is especially true when the shields and calorimeter are much warmer than the cooling tanks since an adequate cooling potential for the shield to stop heating quickly is assured.

Mark IV Control Circuits: The high temperature measurement of heat capacities is achieved through the use of the automatic controls described above over the entire temperature range studied. The major difference between Mark IV and Mark III is that the adiabatic shield is in only two sections. This allows one automatic channel to be used to control the guard shield with support from the ring circuit since no separate floating ring is employed in the thermostat. The guard shield is kept between one and two degrees cooler than the calorimeter to act as a buffer to the outside temperature. As in the low temperature cryostat, adiabatic conditions are maintained to within 0.002°K.

EXPERIMENTAL RESULTS

Method of Calorimetric Measurements and Calculations

For the measurement of an apparent heat capacity of the system under investigation it is necessary to know the initial temperature, T_1, the final temperature, T_2, of a run and the energy, Q, required to traverse this temperature increment. From a knowledge of these quantities the apparent heat capacity will be given by $Q/(T_2-T_1)$ at the mean temperature $(T_2+T_1)/2$.

A platinum-resistance thermometer was used as the thermal sensing device in all measurements. For work done at low temperatures (Mark III) the thermometer (laboratory designation A-3) was calibrated by the National Bureau of Standards from 10°K. to the sulfur point. Below 10° a provisional scale was adopted which follows the resistance of platinum as a function of temperature using an equation of the form $R = A+BT^2+CT^5$. The temperature scale thus defined is believed to agree with the thermodynamic scale to 0.1° below 10°K., 0.03° from 10 to 90°K., and 0.04° from 90 to 350°K. The indicated uncertainties in the temperature pertain only in an absolute sense, and precision and accuracy of temperature increment determinations are considerably better over a normal energy input and are probably reliable to within 0.001° after correction for quasi-adiabatic drift.

The calibration on the platinum-resistance thermometer employed in conjunction with the high temperature measure-

ments (Mark IV) is from 90°K. to the sulfur point. Prior to installation of the thermometer a check was made of the resistance at the triple point of water utilizing the circuits used for heat capacity measurements. This resistance agreed with the calibration value from NBS and was used in the calculation of all temperatures.

The energy increment during an input was calculated from the current through and the voltage across the heater. The trend of voltage with time was assumed to be linear while the change in the current with time was assumed to be no more than quadratic. Under these conditions measurement of the voltage at the middle of an energy input and the current at 21% and 79% of the input duration provides the average value of these current measurements from which an exact evaluation of the energy input may be computed.

Because of the finite temperature change involved it was necessary to correct the value of $Q/(T_2-T_1)$ to the limiting value as (T_2-T_1) approached zero. This is readily done by applying an analytically-determined correction to the observed heat capacities. This correction is normally less than 0.1% except in regions of severe curvature where the method is not applicable.

In the case of studies made in regions of significant vapor pressure, corrections were applied to allow for the heat of vaporization (or sublimation). Appendix I shows the method used for this calculation. Where such corrections for vaporization were necessary the final heat capacities were

those measured under the pressure of saturated vapor, C_s.

Data and Results

Calibration of Intermediate Temperature Thermostat: Although an independent calibration of the thermometer and electrical measuring circuits has been performed, it was considered desirable and indeed necessary to check all calibrations by studying the heat capacity of a well characterized substance. For this purpose the heat capacity of a Calorimetry Conference standard sample of synthetic sapphire,[25] Al_2O_3, was studied from 260-540°K. The sample (187.9554 g. *in vacuo*) was loaded as previously described and a small quantity of helium gas was added for thermal conduction. The results are tabulated in Table I and plotted in Figure 9. Also shown in Figure 9 is the heat capacity of the empty calorimeter used. The calorimeter represents about 20% of the total measured heat capacity at the lower temperature, decreasing to 15% at higher temperatures. The data from this research agree well with that of West and Ginnings[26] whose data are shown by the deviation plot of Figure 10. The zero deviation line represents the best smooth curve through the data of this research with most experimental points falling well within 0.1% deviation limit. It is significant to note that the heat capacities from 500°K. up are more than 0.1% higher than earlier published values of the National Bureau of Standards.[25]

The data ploted in Figure 11 show the effect of nonadiabatic conditions on the subsequent drift. A thermal head was

TABLE I

HEAT CAPACITY OF ALUMINUM OXIDE

(Units: cal., mole, ^{o}K.)

T	C_p	T	C_p
Series I		402.13	23.03
		411.80	23.35
261.55	16.76	421.42	23.61
268.96	17.22		
276.52	17.68	Series II	
284.09	18.11		
291.83	18.54	424.80	23.68
299.93	18.97	434.42	23.94
308.35	19.40	444.05	24.18
317.27	19.83	453.59	24.41
326.42	20.25	463.14	24.63
335.72	20.66	472.70	24.86
345.29	21.05	482.27	25.06
354.80	21.43	491.87	25.20
364.25	21.79	501.39	25.39
373.47	22.06	510.96	25.59
382.96	22.44	520.55	25.77
392.51	22.77	530.21	25.94
		539.56	26.08

Figure 9

Heat Capacity of Aluminum Oxide and

W-22 - Heater - Thermometer - Calorimeter Assembly

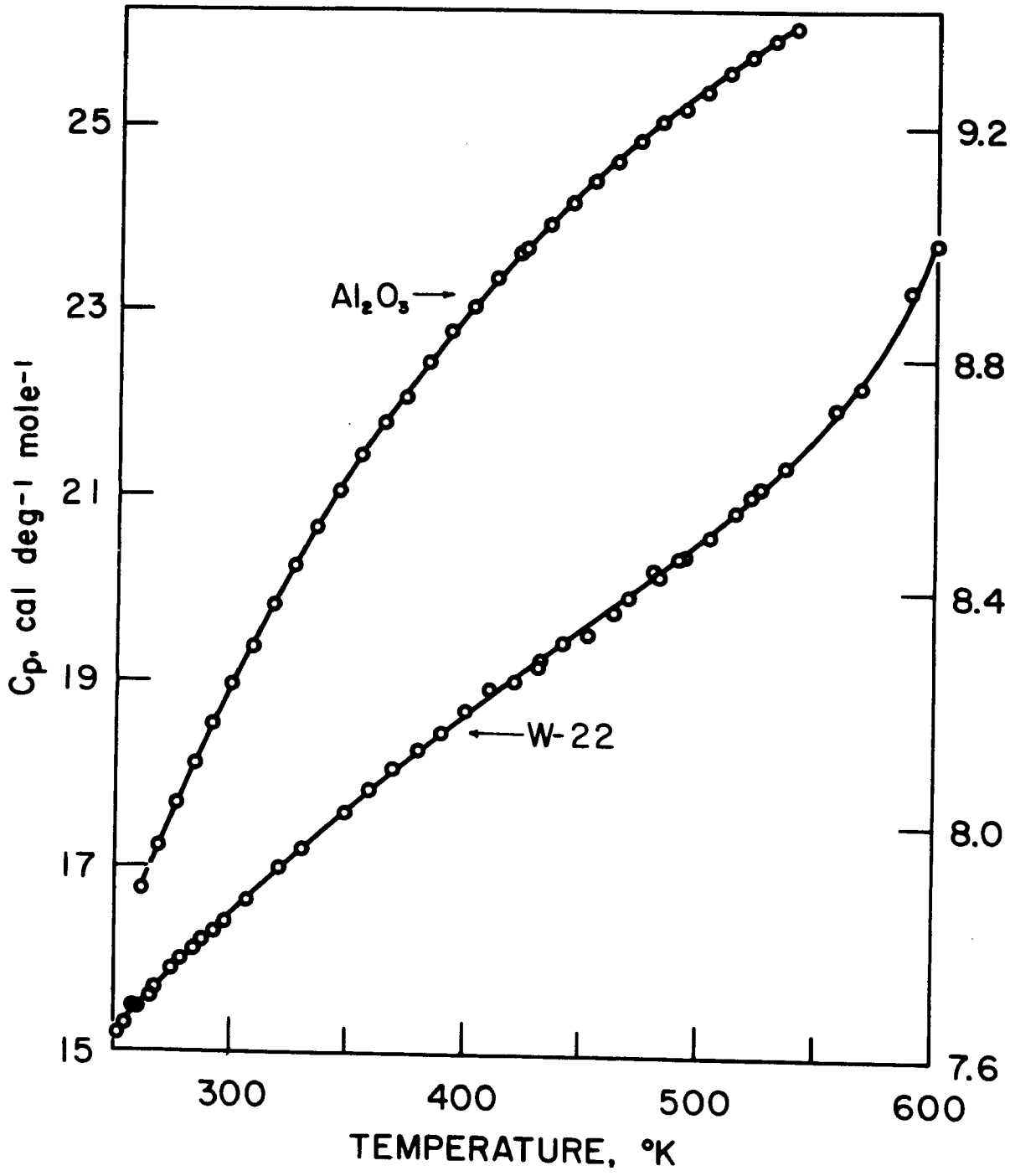

25
23
21
19
17
15
9.2
8.8
8.4
8.0
7.6
C_p, cal deg^{-1} mole^{-1}
Al_2O_3
W-22
300
400
500
600
TEMPERATURE, °K

Figure 9

Figure 10

Deviation from Smooth Curve of This Research

For Aluminum Oxide

Legend:

□ West and Ginnings[24]

○ This research

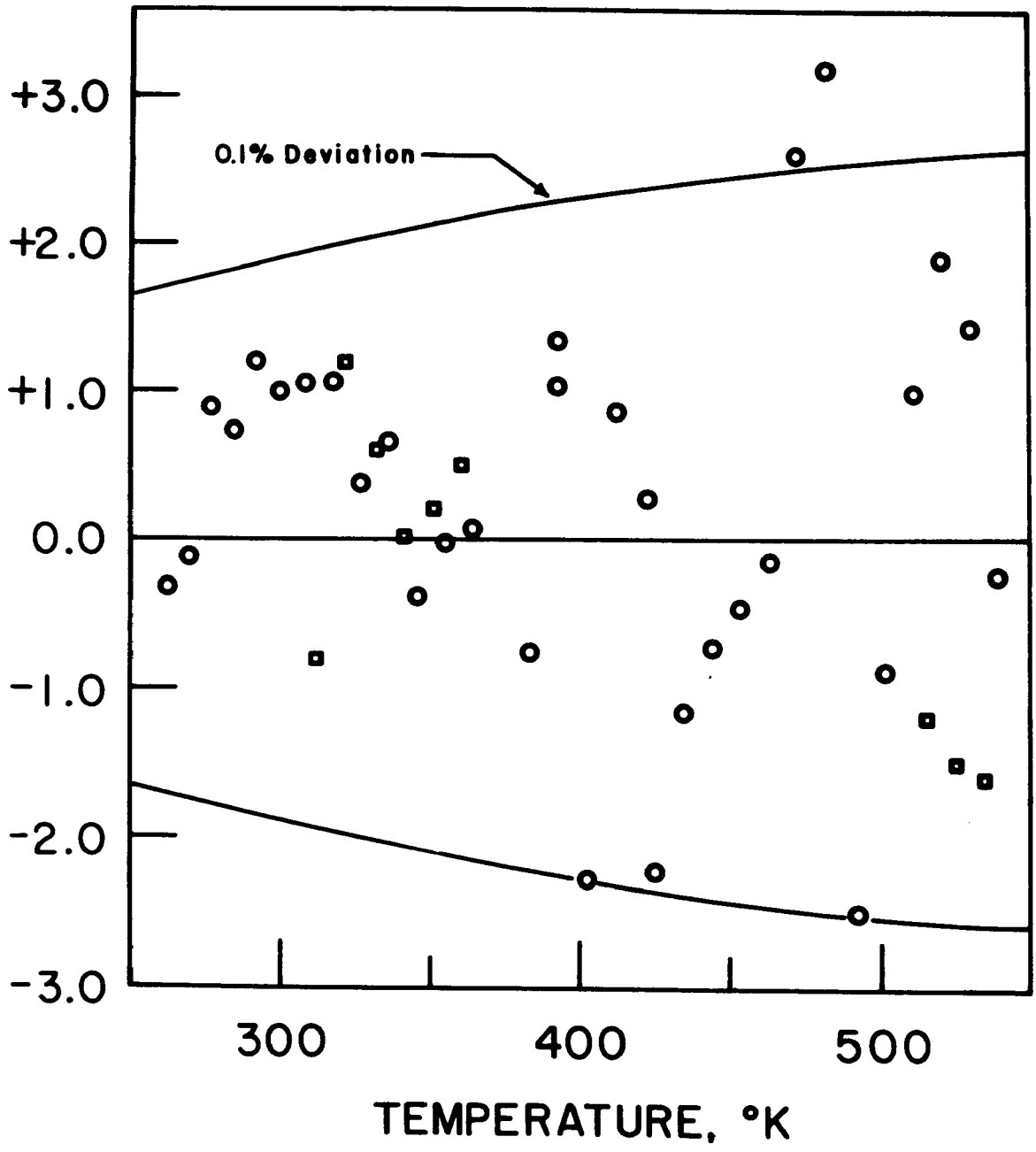


Figure 10

Figure 11

Effect of Thermal Head on Drift

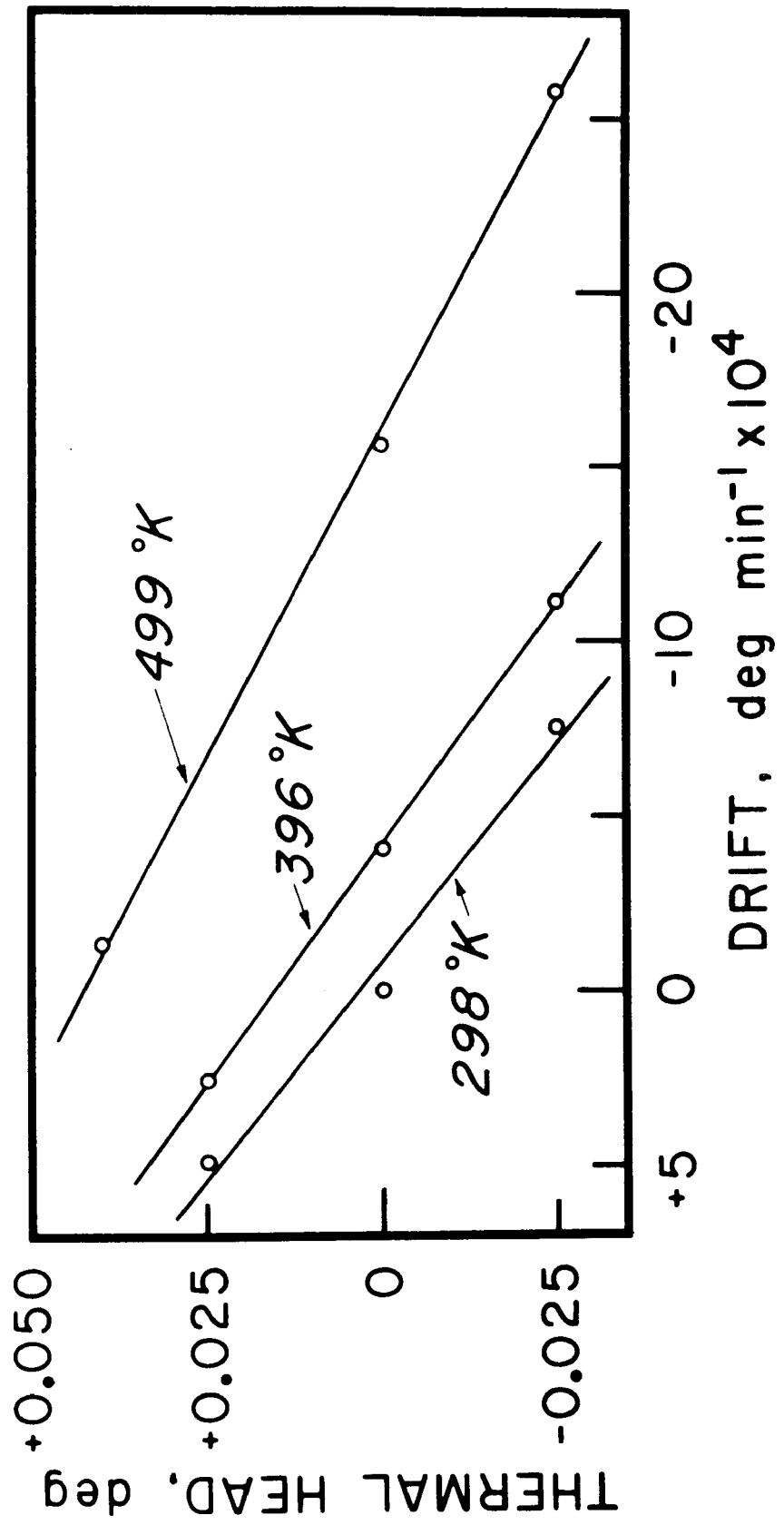

THERMAL HEAD, deg
+0.050
+0.025
0
-0.025
+5
0
-10
-20
DRIFT, deg min^{-1} x 10^4
499 °K
396 °K
298 °K

Figure 11

caused by controlling the cylindrical top-middle adiabatic shield at a small temperature increment away from null. Under such conditions the thermal leakiness modulus, defined as the ratio of the time rate of change of temperature to thermal head, may be computed. The modulus, λ, for the system under study takes on a linear dependence with temperature which can be best expressed by the relation $\lambda = 4.3 \times 10^{-3} - 8.17 \times 10^{-5} T$ in units of $min.^{-1}$. From the results of this study it was possible to assure a near zero drift over the entire temperature range covered by judicious adjustment of the top-middle adiabatic shield. Utilization of the thermal leakiness modulus permitted the calculation that an uncertainty in the adiabaticity of $0.002^{\circ}K.$ amounted to some 0.06% of the Al_2O_3 heat capacity for a typical 50-minute experiment at $400^{\circ}K.$ This 0.06% is comparable to the observed scatter in the data in this temperature region shown by the deviation plot of Figure 10 and serves to point up the considerable heat effect from so small a temperature difference.

Triethylenediamine (1,4-diazabicyclo [2,2,2] octane): Work from this laboratory initiated by Chang and Westrum[27] shows the onset of a transition just beyond the range of the cryostat used and well within the range of the Mark IV thermostat. The study of this transition and fusion was carried out using the same sample employed in the earlier low temperature studies. The experimental heat capacity determinations are presented in Table II in chronological order in terms of

TABLE II

HEAT CAPACITY OF TRIETHYLENEDIAMINE

(Units: cal., mole, °K.)

T	C_s
Series I	
302.43	37.06
311.66	38.74
321.34	40.65
331.10	42.86
340.79	45.50
TRANSITION RUNS A	
358.51	50.58
368.74	51.46
378.97	52.23
389.42	53.16
400.02	54.20
410.64	55.19
421.28	56.35
FUSION RUNS B	
427.62	57.51
Series II	
320.03	40.09
326.63	41.62
334.36	43.62
341.64	45.64
347.60	47.83
TRANSITION RUNS C	
355.29	50.16
358.30	50.31
359.55	50.40
363.97	51.00
372.45	51.67
381.18	52.46
389.34	53.19
397.65	53.95
407.03	54.83
416.34	55.81
423.61	56.33
428.66	56.56
429.60	56.96
430.54	56.76
431.64	57.91
432.44	64.55
FUSION RUNS D	
434.59	57.37
436.25	57.24
438.94	57.78
Series III	
344.76	46.38
348.09	47.74
349.94	47.88
TRANSITION RUNS E	
ENTHALPY RUN F	
FUSION RUN G	
Series IV	
299.89	36.44
303.33	37.14
308.09	37.94
311.43	38.66
319.33	40.23
328.56	42.09
338.18	44.82
TRANSITION RUN H	
Series V	
354.02	49.86
357.49	50.54
365.80	51.26
376.83	52.20
Series VI	
FUSION RUNS J	
Series VII	
433.66	57.23
434.19	57.26
434.54	57.26
435.07	57.47
438.21	57.70
441.91	57.96
443.80	58.19
445.83	58.36
448.01	58.64
Series VIII	
TRANSITION RUNS K	
383.49	52.70
Series IX	
FUSION RUNS L	

TABLE II (Cont.)

TRANSITION INCREMENTS			FUSION INCREMENTS		
T	Δ T	Apparent C_s*	T	Δ T	Apparent C_s*
	RUNS A			RUNS B	
348.34	5.433	(97.22)	429.82	6.414	(104.3)
351.06	0.058	13400	433.01	0.018	454
351.13	0.131	7030	433.71	1.405	(524.5)
352.21	2.279	(288.1)			
	RUNS C			RUNS D	
			432.79	0.207	175
350.58	0.970	301	433.61	1.416	(1291)
351.09	0.102	15800			
351.16	0.156	3010		RUNS J	
352.04	1.762	(157.5)			
			432.38	1.212	(515.8)
	RUNS E		432.99	0.015	52500
			434.48	2.973	(202.2)
350.69	0.528	97.8			
351.86	1.826	(1413)		RUNS L	
	RUNS K		(cf. TABLE III)		
350.67	0.300	82.1			
364.44	27.23	(98.10)			

* Values in parenthesis emphasize that due to large Δ T's, these values are Q/ΔT's and do not necessarily represent true heat capacities.

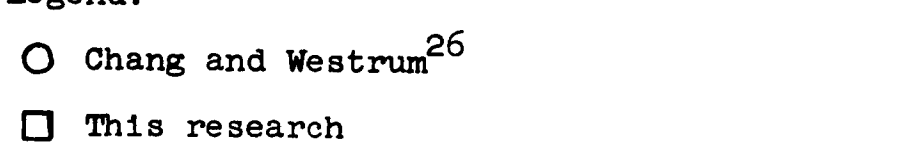
the thermochemical calorie defined as exactly 4.184 abs. j. The ice point was taken as 273.15°K. and the molecular weight of triethylenediamine as 112.172 g. The calorimeter was loaded in an anhydrous nitrogen atmosphere with a 70.3256 g. (in vacuo) sample by heating the calorimeter to fuse the sample, allowing a greater quantity to be used. The calorimeter was evacuated and filled with 10 cm. Hg pressure of purified He gas at 300°K. to enhance the thermal contact between sample and calorimeter.

Corrections to the observed values of $\Delta H/\Delta T$ were applied for the sublimation or vaporization of the sample at higher temperatures and for the analytically-determined curvature correction when applicable. These corrections have maximum magnitudes of approximately 0.03 % and 0.01% respectively. The approximate increments used in the measurements can usually be inferred from the adjacent mean temperatures in Table II. The molal experimentally determined heat capacities are shown graphically in Figure 12.

The sharp and seemingly first-order transition at 351.08°K. is characterized by apparent heat capacities as high as 15,800 cal. $mole^{-1}$ $^{o}K.^{-1}$ and thermal equilibrium within an hour after energy input. If the lattice contributions to the heat capacity (obtained by extrapolation through the transition of the normal heat capacity) are deducted from the apparent heat capacities, a transitional enthalpy increment of 2524.0 cal. $mole^{-1}$ and a corresponding entropy increment of 7.19 cal. $mole^{-1}$ $^{o}K.^{-1}$ are obtained. These represent minimal values

Figure 12

Heat Capacity of Triethylenediamine



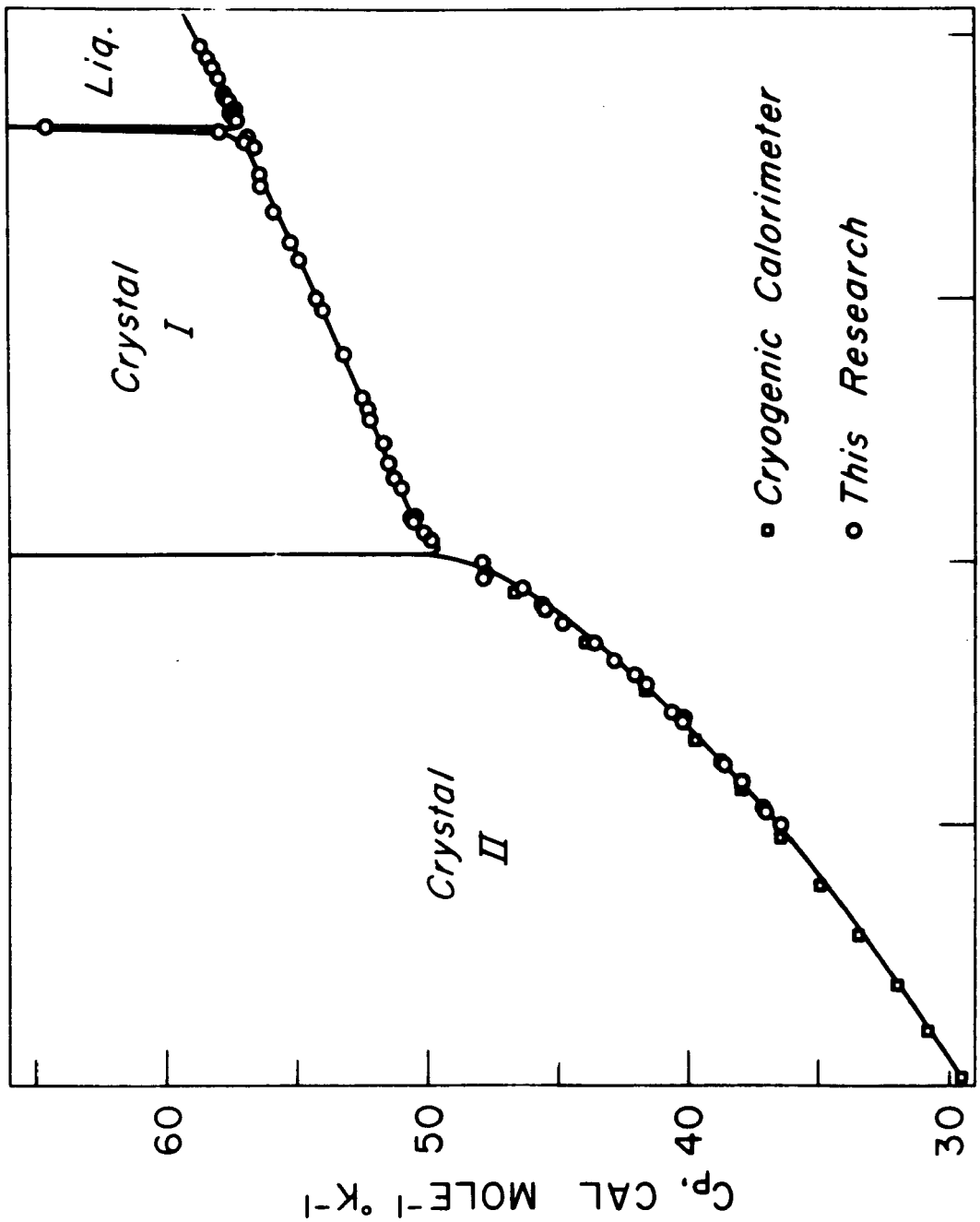

Liq.
Crystal I
Crystal II
▫ Cryogenic Calorimeter
○ This Research
Cp, CAL MOLE⁻¹ °K⁻¹
60
50
40
30
250
300
350
400
450
T, K

Figure 12

since a maximum lattice heat capacity has probably been assigned.

Fusion occurs at 432.98°K. yielding an enthalpy increment of 1776.5 cal. mole^{-1} and an entropy increment of 4.10 cal. mole^{-1} °K.$^{-1}$. Molal heat capacities as high as 58,000 cal. mole^{-1} °K.$^{-1}$ were observed in the fusion region with thermal equilibrium being readily attained within one hour.

The near absence of premelting suggests the applicability of the method of Tunnicliff and Stone[27] for the determination of sample purity. The data used for triethylenediamine is listed in Table III where F is the fraction melted. The straight line plot of the reciprocal fraction melted versus absolute temperature (Figure 13) implies no solid solution formation and indicates 0.003 mole percent solid-insoluble impurity for this sample. Extrapolation of this plot also furnishes the true melting point of this sample and the melting point of a pure sample as 432.983°K. and 432.990°K., respectively. Chemical microanalysis of the triethylenediamine sample studied gave the following composition: 64.39% C, 10.81% H and 24.75% N(calculated: 64.24% C, 10.78% H and 24.96% N for $C_6H_{12}N_2$).

The thermodynamic functions given in Table IV were obtained from the heat capacity data by integration of a least squares fitted curve through the experimental points and numerical quadrature thereof by a high-speed digital computer. Corrections for neither nuclear spin nor isotopic mixing were made to the entropy or free energy functions; hence

TABLE III

FRACTIONAL FUSION OF TRIETHYLENEDIAMINE

(Units: cal., mole, °K.)

T_{mean}	ΔT	C_s	ΔH_{excess}	$1/F$	T_{final}
		FUSION RUNS L			
430.463	4.953	69.13	60.9	29.153	432.909
432.936	0.054	7530	468.5	3.791	432.964
432.968	0.009	42530	856.7	2.074	432.973
432.976	0.007	58230	1294.2	1.373	432.980
432.981	0.002	1690	1749.1	1.016	432.982
433.541	1.048	70.37	1776.7		434.030
		Melting Point: This Sample		(1.000)	(432.983)
		Melting Point; Pure Compound		(0.000)	(432.990)

Figure 13

Fractional Fusion Curve for Triethylenediamine

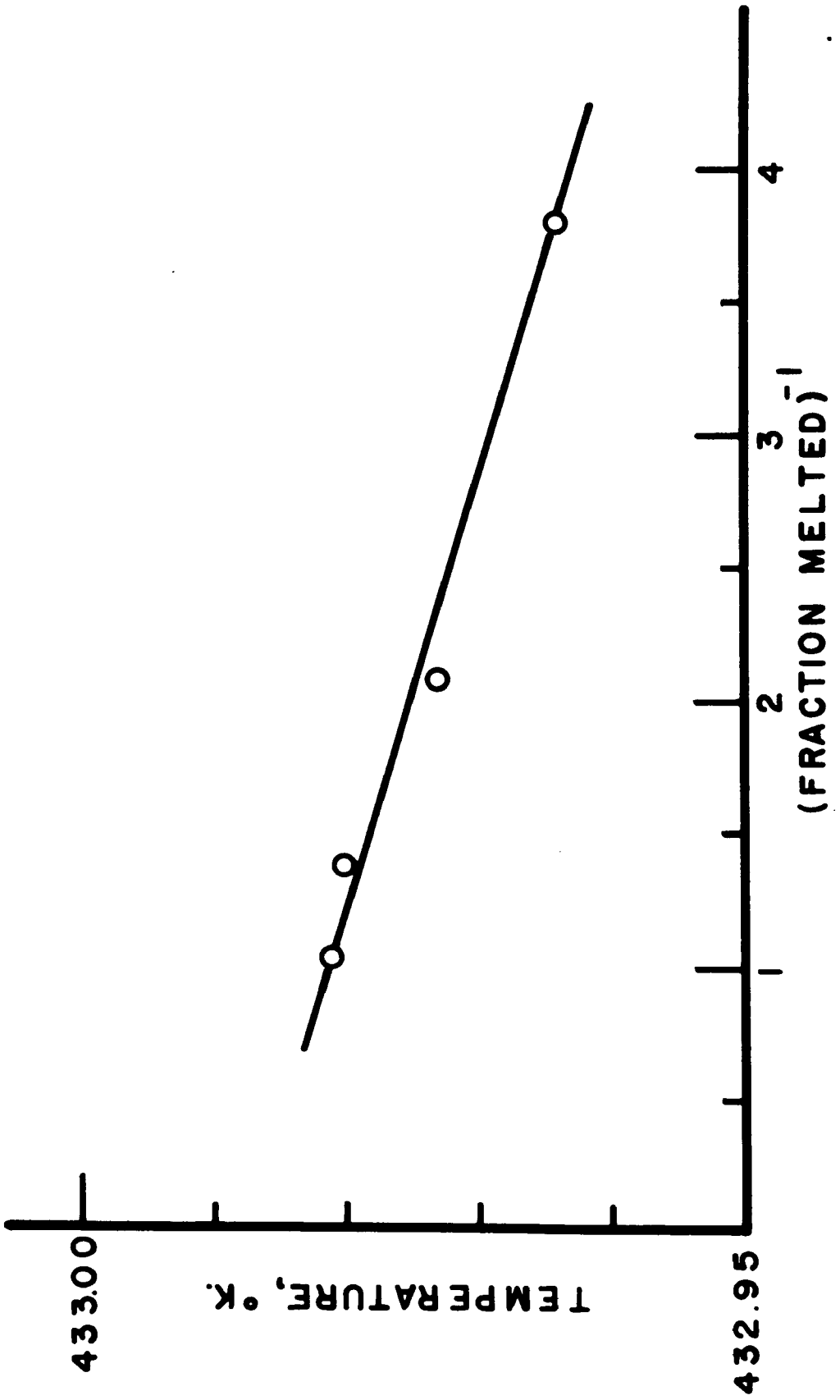


Figure 13

TABLE IV

THERMODYNAMIC FUNCTIONS OF TRIETHYLENEDIAMINE

($C_6H_{12}N_2$; 1 mole = 112.172g.; Units: cal., mole, °K.)

T	C_s	S^o	$H^o-H_o^o$	$-(F^o-H_o^o)/T$
		CRYSTAL II		
298.15*	36.49	37.67	5524.8	19.14
300	36.80	37.90	5592.6	19.25
320	40.35	40.38	6363.1	20.50
340	45.13	42.96	7214.7	21.74
351.09	(48.80)	44.43	7723.3	22.43
		CRYSTAL I		
351.09	(49.90)	51.61	10244	22.43
360	50.62	52.90	10707	23.16
380	52.34	55.69	11737	24.80
400	54.17	58.42	12802	26.42
420	56.04	61.11	13904	28.00
432.98	(56.90)	62.84	14636	29.04
		LIQUID		
432.98	(57.16)	66.95	16412	29.04
440	57.83	67.86	16817	29.64
450	58.79	69.17	17400	30.50

* From Chang and Westrum[26]

these are practical values for thermochemical calculations.

A final check on over-all precision was obtained by making enthalpy-type measurements over both anomalous regions and over a range of normal heat capacity between the two transitions. Enthalpies obtained from these latter runs accord very favorably with that integrated from heat capacity data over the Crystal I region as shown in Table V which also shows the data spanning the two transition regions. The listed enthalpy changes in these regions are a direct summation of the energies used while entropy increments have been integrated from heat capacity data except in regions of extremely high heat capacities where the process is assumed to be isothermal.

Pentaerythrityl Fluoride: Earlier work on the thermodynamics of pentaerythritol and its halide derivatives[29,30] indicated the fluoride to be particularly interesting. By studying the fusion thermal effects a basis would be available for the correlation of the solid state transition in pentaerythrityl fluoride with that in pentaerythritol and would give an added check to the proposed mechanism of the transition in the former. Since the lower temperature studies had been completed on the fluoride, Mark IV was utilized to investigate the compound through its melting point. The identical sample was used also for the higher temperature work to make all measurements consistent. The sample had been carefully stored in a sealed glass tube which was open-

TABLE V

ENTHLPY AND ENTROPY INCREMENTS OF TRIETHYLENEDIAMINE

(Units: cal., mole, ^{o}K.)

Designation	Energy Increments	T_{final}	$T_{initial}$	$H^{o}_{355}-H^{o}_{345}$	$S^{o}_{355}-S^{o}_{345}$
		TRANSITION			
Series II	7	357.66	338.18	3011.1	8.569
Runs A*	4	353,35	345,62	(3008.3)	(8.561)
Run H	1	354.29	342.96	3010.6	8.568
Runs K	2	378.06	350.54	3010.9	8.568
			Average	3010.9	8.568
		FUSION			
				$H^{o}_{440}-H^{o}_{430}$	$S^{o}_{440}-S^{o}_{430}$
Series II	9	440.81	429.98	2348.4	5.423
Runs B*	4	440.84	426.61	(2352.9)	(5.433)
Run G	1	435.97	429.34	2350.1	5.428
Runs J	3	439.97	431.78	2348.2	5.423
Runs L	6	434.03	427.99	2349.8	5.427
			Average	2349.1	5.425
		CRYSTAL I			
				$H^{o}_{430}-H^{o}_{355}$	
Series I	7	426.60	353.36	4010.4	
Series II	16	431.09	352.91	4009.8	
Run F	1	429.38	352.77	4014.3	
			Average	4011.5	
Numerical Quadrature of Smoothed Curve:				4013.1	

* Rejected from average by Chauvenet's criterion.

ed in an anhydrous nitrogen atmosphere where all the loading operations were carried out. The calorimeter and sample were warmed and the sample was poured as a liquid into the calorimeter where it was allowed to cool. For these measurements 58.6279 g. (in vacuo) of pentaerythrityl fluoride were used. Table VI lists the experimental heat capacities in chronological order in terms of the ice point as 273.15°K. and the defined thermo-chemical calorie as 4.184 abs. j. The molecular weight of pentaerythrityl fluoride was taken as 144.119 g. For thermal conduction 12.5 cm. Hg pressure of helium gas at 300°K. was put into the sample space before sealing off the calorimeter.

Corrections (which amounted to less than 0.01% over the entire temperature range investigated) were applied to the data for finite temperature increments. No correction was made for sublimation or vaporization since no adequate representation of the vapor pressure as a function of temperature was available. However, this emendation is estimated to be less than 0.05%. Figure 14 is a plot of the experimentally-determined heat capacities showing also some of the low temperature work. The nearly 0.2% discrepency in the measured heat capacities in the two apparatuses at the point of overlap has a negligible effect on the thermodynamic functions.

The first-order fusion transition occurs at 367.06°K. yielding an enthalpy increment of 1229.8 cal. $mole^{-1}$ which corresponds to an entropy increment of 3.347 cal. $mole^{-1}{}^{o}K.^{-1}$.

TABLE VI

HEAT CAPACITY OF PENTAERYTHRITYL FLUORIDE

(Units: cal., mole, °K.)

T	C_s	T	C_s	Fusion Increments T	ΔT	Apparent C_s*
Series I		Series IV		RUNS A		
301.31	50.67	FUSION RUN D		359.43	10.293	(56.17)
309.07	51.37			365.39	1.682	(165.1)
319.34	52.12	Series V		366.46	0.523	576
329.28	52.91			366.80	0.213	1440
339.28	53.70	FUSION RUNS E		366.99	0.164	1970
349.19	54.63			368.08	1.954	(139.4)
FUSION RUNS A		Series VI		RUNS C		
		369.18	59.83			
371.04	60.80	369.99	60.30	(cf. TABLE VII)		
374.97	61.09	373.39	60.99			
		377.85	61.15	RUNS E		
Series II		381.04	61.36			
				367.02	0.030	1450
ENTHALPY RUN B		Series VII		367.04	0.023	1900
				367.05	0.024	1790
FUSION RUNS C		300.98	50.71	367.07	0.026	1690
		308.62	51.27	367.09	0.026	1660
371.13	60.74	317.15	51.90			
374.93	61.07	326.40	52.65			
		335.74	53.44			
Series III		345.08	54.30			
		354.38	55.15			
362.88	56.64	360.82	56.05			
363.75	62.83					
364.35	73.13	Series VIII				
		FUSION RUN F				

* Values in parenthesis emphasize that due to large ΔT's, these values are Q/ΔT's and do not necessarily represent true heat capacities.

Figure 14

Heat Capacity of Pentaerythrityl Fluoride

Legend:

○ Payne[30]

□ This research

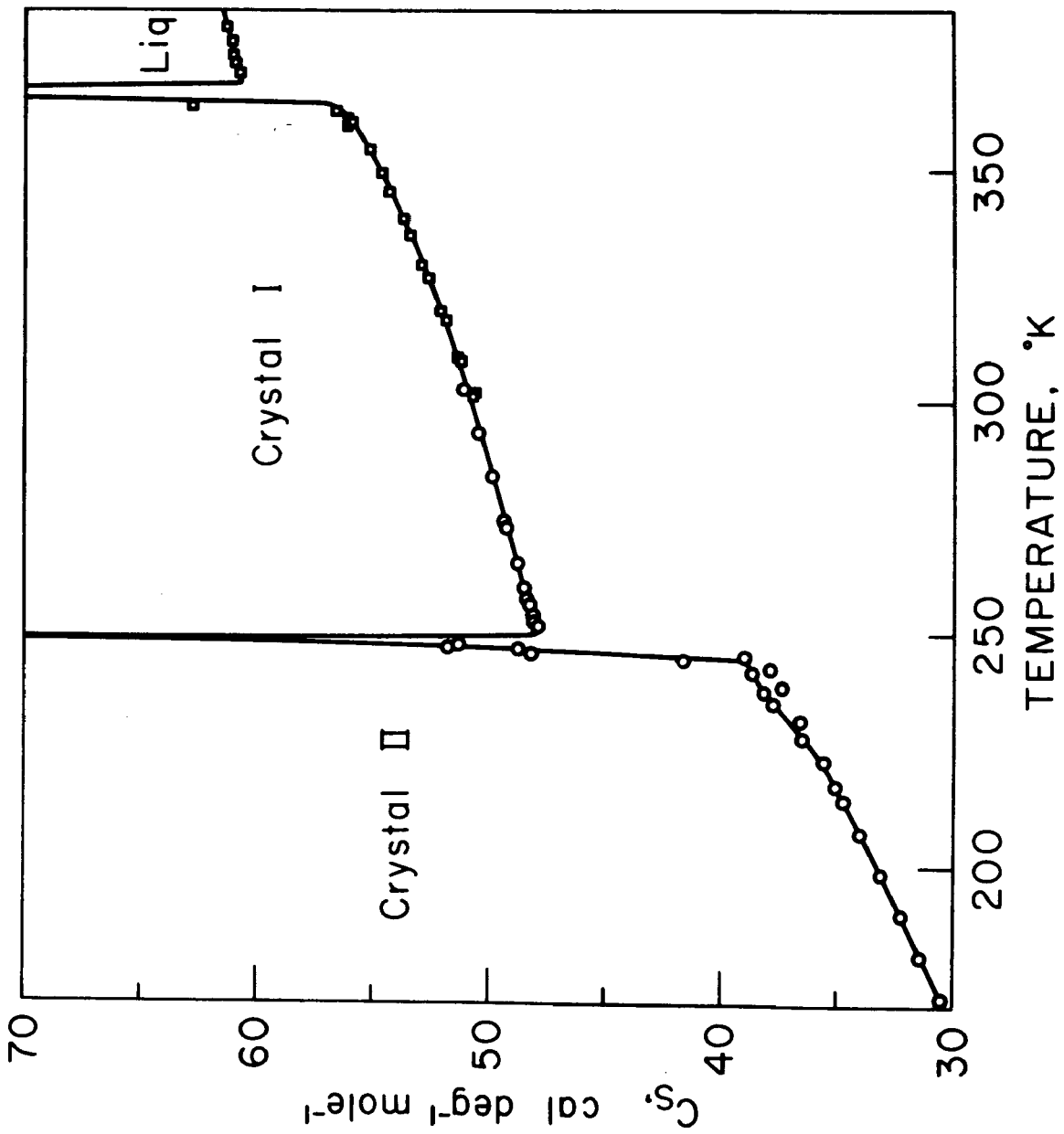

Liq
Crystal I
Crystal II
70
60
50
40
30
200
250
300
350
TEMPERATURE, °K
C_s, cal deg^{-1} mole^{-1}

Figure 14

Equilibrium through the fusion region was rather slow. Up to 3.5 hours were required to attain the normal equilibrium drift. Molal heat capacities as high as 1900 cal. $mole^{-1}$ $^{o}K.^{-1}$ were observed.

Utilizing the fractional melting data from Table VII for this sample of pentaerithrityl fluoride, Figure 15 shows that a plot of reciprocal fraction melted versus temperature is not a straight line. This behavior suggests that the impurity forms a solid solution with the sample. Applying the method of Mastrangelo and Dornte[31] to correct for the presence of solid solution, it was calculated that the sample contained 0.18 mole percent impurity. Furthermore, it was possible to calculate the melting point of this sample as 367.06°K. and that of a pure sample as 367.43°K.

The thermodynamic properties calculated by quadrature of the experimental heat capacity data on a digital computer are provided at selected temperatures in Table VIII. Nuclear spin and isotopic mixing contributions have not been included in the entropy or in the free energy function. The tabulated functions are based on the low temperature values for the enthalpy and entropy obtained by Payne[30] below 300°K.

An added check on the fusion anomaly was obtained by making several enthalpy-type runs through the entire fusion region. A comparison of these measurements with the normal heat capacity measurements in this region is shown in Table IX. Enthalpy-type measurements are also given over a normal heat capacity region. The listed enthalpy changes in the fu-

TABLE VII

FRACTIONAL FUSION OF PENTAERYTHRITYL FLUORIDE

(Units: cal., mole, °K.)

T_{mean}	ΔT	C_s	ΔH_{excess}	1/F	T_{final}
		FUSION RUNS C			
364.540	0.588	74.21	21.53	56.062	364.834
364.927	0.248	92.06	32.69	36.920	365.052
365.520	0.985	176.5	153.11	7.884	366.012
366.322	0.620	477.9	411.71	2.932	366.612
366.758	0.259	1170	699.42	1.726	366.888
368.056	2.339	257.4	1227.05		369.226
			Melting Point; This Sample	(1.000)	367.057
			Melting Point; Pure Compound	(0.000)	367.427

Figure 15

Fractional Fusion Curve for Pentaerythrityl Fluoride

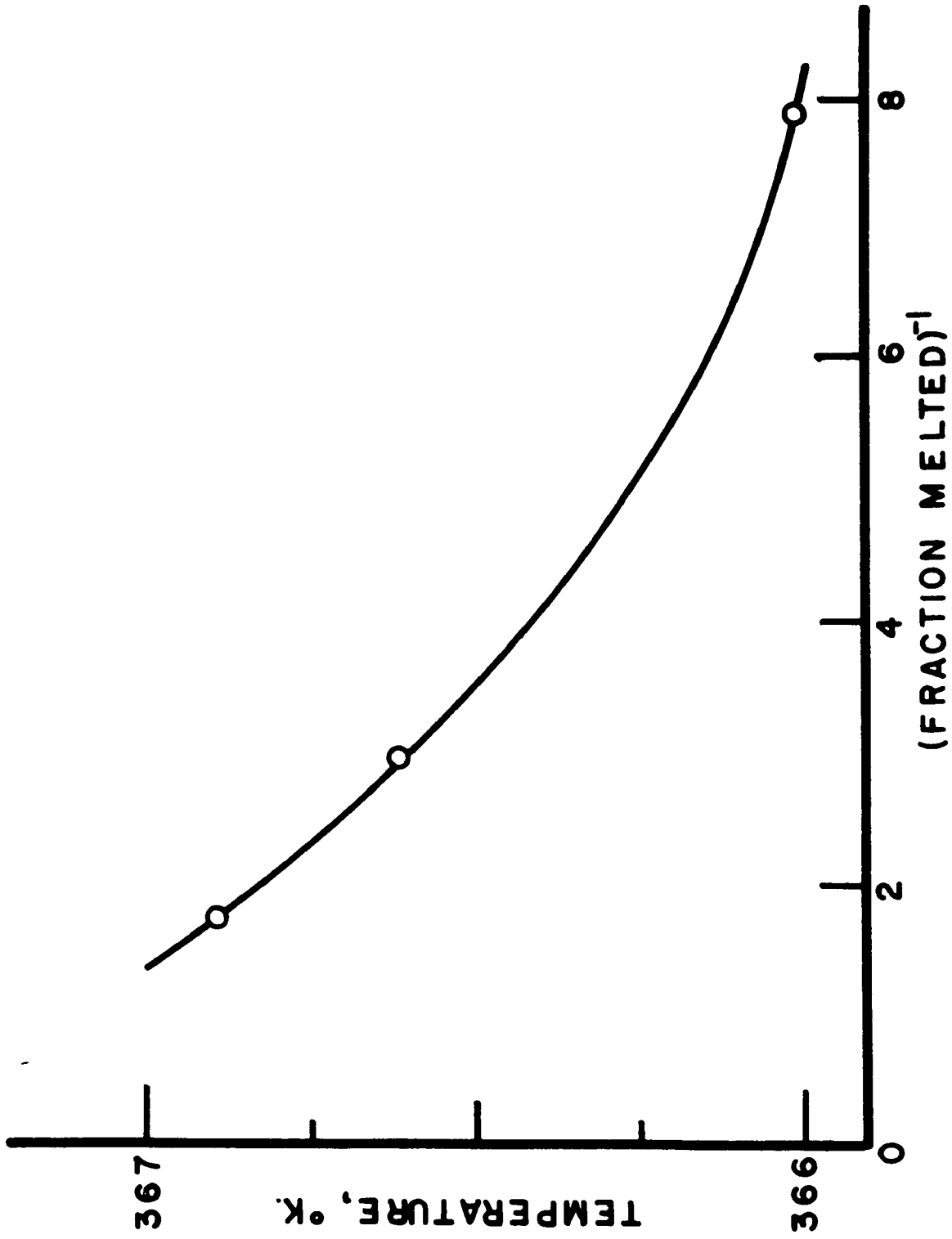


Figure 15

TABLE VIII

THERMODYNAMIC FUNCTIONS OF PENTAERYTHRITYL FLUORIDE

($C_5H_8F_4$; 1 mole = 144.119g.; Units: cal., mole, °K.)

T	C_s	S°	$H^\circ-H_0^\circ$	$-(F^\circ-H_0^\circ)/T$
		CRYSTAL I		
298.15*	50.71	69.31	11333	31.30
300	50.82	69.63	11427	31.53
310	51.47	71.30	11939	32.79
320	52.15	72.95	12457	34.02
330	52.91	74.56	12982	35.22
340	53.76	76.16	13515	36.40
350	54.76	77.73	14058	37.56
360	55.94	79.27	14611	38.69
367.06	(56.84)	80.45	15030	39.50
		LIQUID		
367.06	(60.61)	83.80	16259	39.50
370	60.69	84.21	16413	39.81
380	61.31	85.83	17024	41.03

* From Payne[29]

TABLE IX

ENTHALPY AND ENTROPY INCREMENTS OF

PENTAERYTHRITYL FLUORIDE

(Units: cal., mole, ^{o}K.)

Designation	Energy Increments	T_{final}	$T_{initial}$	$H^{o}_{375}-H^{o}_{355}$	$S^{o}_{375}-S^{o}_{355}$
		FUSION			
Series I	8	376.89	354.28	2387.7	6.518
RUNS C*	9	376.82	364.25	(2367.1)	(6.462)
RUN D	1	369.17	362.68	2381.7	6.502
RUN F	1	374.80	353.21	2385.2	6.511
		Average		2384.9	6.510
		CRYSTAL I			
				$H^{o}_{360}-H^{o}_{330}$	
Series I	3	364.57	334.46	1629.0	
Series VI	4	362.64	331.07	1629.2	
RUN B	1	364.26	328.38	1629.2	
		Average		1629.1	
Numerical Quadrature of Smoothed Curve:				1629.0	

* Rejected from average by Chauvenet's criterion.

sion region are a direct summation of the energies used while entropy increments have been integrated from heat capacity data except in regions of extremely high heat capacities where the process is assumed to be isothermal.

Perchloric Acid: The perchloric acid sample used for calorimetric investigation was prepared by the methods of G.F. Smith.[13] Two precautions were rigorously observed: (1) complete exclusion of any oxidizable material including vapor as well as solid and liquid contaminants, and (2) adequate temperature control, for should the distillation reservior, or any other place where perchloric acid vapors are present, be heated too strongly a vapor phase decomposition will take place[32] which will pollute the desired product. For the above mentioned reasons the preparation was carried out in an all glass vacuum line containing no stopcocks or valves. In order to produce a sufficiently large sample 1000 cc. of 20-23% fuming sulfuric acid (reagent grade) were added to a 3000 cc. distilling flask which contained 260 cc. double distilled 70% perchloric acid. The vacuum line was then sealed, cooled to 5°C. and evacuated. At a pressure of 0.05 mm. Hg and 10°C. perchloric acid ebulated readily and was collected as a liquid in a trap cooled by a dry ice-isopropanol slush. The distillation flask was heated slowly to 50°C. with a heating mantle controlled by an auto transformer and sealed from the line without loss of vacuum. A liquid nitrogen trap prevented the decomposition products accumulated dur-

ing seal-off from contaminating the perchloric acid. About 100 cc. of product were obtained which were distilled twice prior to the final distillation into the glass calorimeter liner. To assure ready attainment of thermal equilibrium 14.4 mm. Hg pressure of purified helium gas at 80°K. was added to the liner before removing it from the line. The sample (72.7128 g. in vacuo) and sealed liner were placed in a gold-plated calorimeter (laboratory designation W-33) where the void space between components was filled with 17.8 cm. Hg pressure of helium gas at 300°K. The experimental heat capacities are listed in Table X and shown graphically in Figure 16. The approximate temperature increment can usually be inferred from the mean temperature of the adjacent runs in Table X. All heat capacities are in terms of the defined thermochemical calorie as 4.184 abs. j., the ice point as 273.15°K. and the molecular weight of perchloric acid as 100.465 g. Adjustment of the observed $\Delta H/\Delta T$ for curvature was applied and had a maximum value of 0.2% below 15°K., decreasing rapidly to 0.01% over the rest of the temperatures investigated. No correction for vaporization was necessary since a sample calculation at the highest temperature studied showed a correction of less than 0.01%.

Fusion, which occurs at 171.13°K., was accompanied by an enthalpy change of 1657.0 cal. mole^{-1} and an entropy increment of 9.68 cal. mole^{-1} °K.$^{-1}$. This first-order transition showed a great deal of apparent premelting even though heat capacities as high as 1820 cal. mole^{-1} °K.$^{-1}$ were observed.

TABLE X

HEAT CAPACITY OF PERCHLORIC ACID

(Units: cal., mole, °K.)

T	C_p	T	C_p
	Series I	Heated to 180.69 °K.	
6.64	0.065		Series IV
7.18	0.092		
7.97	0.129	144.08	15.83
8.92	0.203	150.55	16.39
9.98	0.306	156.16	16.96
11.14	0.427	161.13	18.57
12.37	0.576	164.99	21.43
13.65	0.776	167.63	37.97
15.06	1.016		
16.68	1.329		Series V
18.52	1.712		
20.59	2.170		FUSION RUN A
	Series II		Series VI
20.83	2.226	86.55	11.54
23.18	2.775	93.60	12.05
25.99	3.437	100.90	12.56
29.01	4.131	108.51	13.11
32.24	4.852	116.24	13.67
35.75	5.583	124.39	14.30
39.26	6.250	132.61	14.94
42.93	6.869	139.72	15.50
47.10	7.531	146.54	16.05
51.99	8.201	153.23	16.65
57.33	8.853	158.78	17.71
63.01	9.474	163.55	20.08
69.14	10.05	167.03	28.21
75.93	10.64		
83.38	11.28		FUSION RUNS B
	Series III	176.10	26.05
		178.64	26.07
82.11	11.18	181.78	26.10
90.40	11.83		
99.25	12.44		Series VII
108.11	13.08		

TABLE X (Cont.)

T	C_p	T	C_p
FUSION RUN C		Series XII	
178.44	26.05	113.88	13.51
Series VIII		123.32	14.21
		132.08	14.87
ENTHALPY RUN D		140.40	15.55
		148.36	16.18
FUSION RUN E		155.88	16.94
		162.66	19.68
178.83	26.10	167.43	46.42
184.49	26.16		
Series IX		Series XIII	
		FUSION RUN H	
FUSION RUN F		186.82	26.19
		195.30	26.34
Series X		204.02	26.52
		212.90	26.68
173.27	26.05	221.90	26.84
176.40	26.16	231.31	27.08
		240.97	27.28
Series XI		250.53	27.49
		259.78	27.78
FUSION RUNS G		268.60	27.95
		277.54	28.19
177.77	26.06	286.41	28.47
		295.14	28.68

Figure 16

Heat Capacity of Perchloric Acid

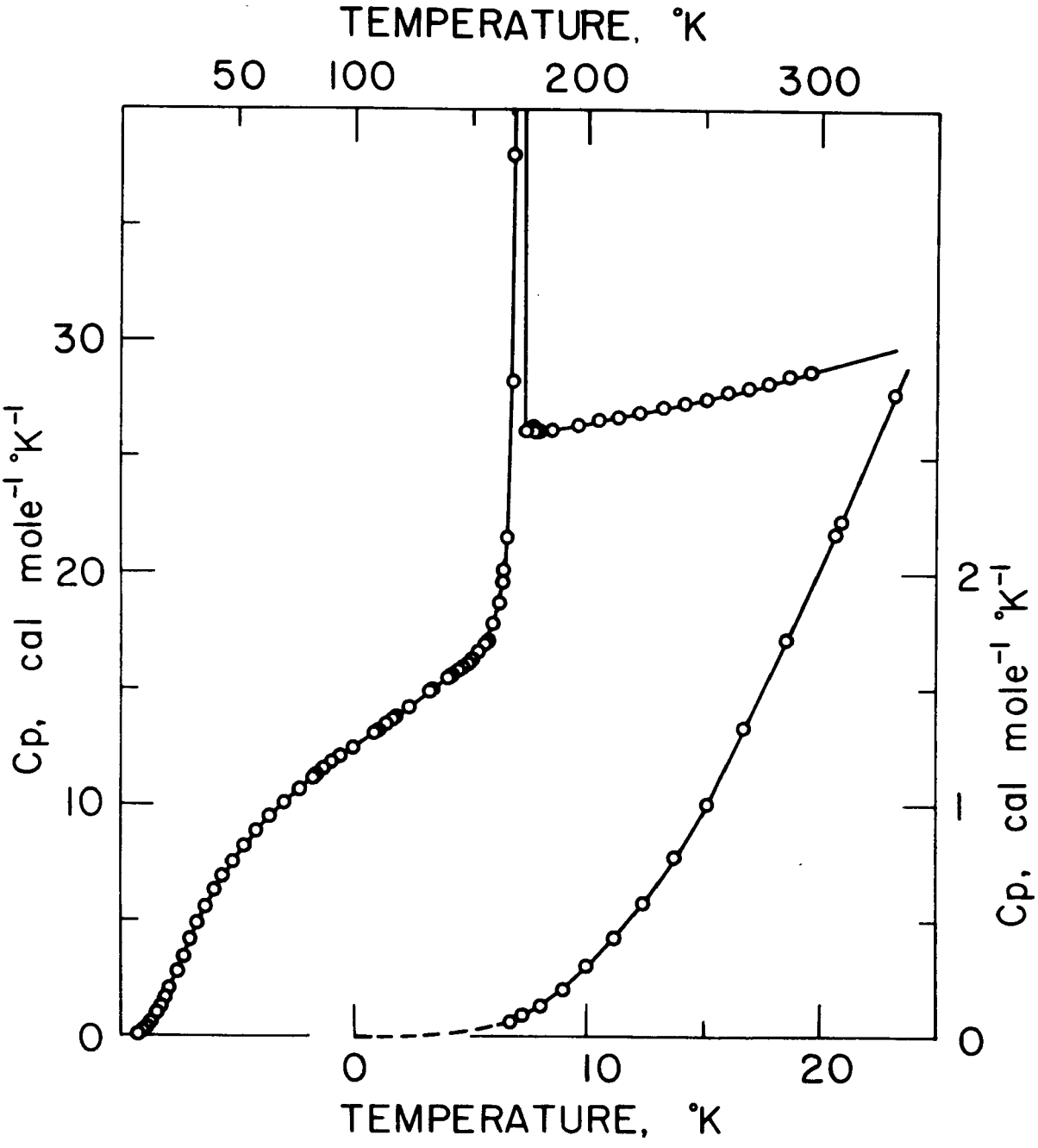

TEMPERATURE, °K
50
100
200
300
30
20
10
0
Cp, cal mole⁻¹ °K⁻¹
2
1
0
0
10
20
TEMPERATURE, °K
Cp, cal mole⁻¹ °K⁻¹

Figure 16

Table XI and Figure 17 show in detail the fractional melting data from two separate series of runs which were used to calculate purity and melting point. The method of Mastrangelo and Dornte[31] was employed for this calculation showing an impurity of 2.5 mole percent presumed to be perchloric acid monohydrate. A complete analysis of this phenomena will be found in the discussion section for perchloric acid. The melting point of this sample was found to be 171.13°K. and that of a pure sample as 172.01°K.

The molal thermodynamic functions are listed at selected temperatures in Table XII. The values were obtained by digital computer integration of a least squares fit polynomial through the experimental data points. The smooth heat capacities obtained were essentially identical to those obtained from a large scale plot. The data were extrapolated below 5 °K. with a Debye T^3 relationship. The entropies and free energy functions do not include contributions from nuclear spin or isotopic mixing and are hence practical values for chemical thermodynamic purposes.

As a confirmative test of the precision of the calorimetry and heat capacity-type runs in the transition region, several enthalpy increments, each covering the anomalous region, were made and are compared with integrated heat capacity determinations in Table XIII. The agreement is quite satisfactory.

TABLE XI

FRACTIONAL FUSION DATA OF PERCHLORIC ACID

(Units: cal., mole, $^{o}K.$)

T_{mean}	ΔT	Apparent C_s	ΔH_{excess}	$1/F$	T_{final}
		FUSION RUNS B			
168.830	1.035	284.4	316.50	5.238	169.348
169.765	0.835	352.0	594.92	2.787	170.182
170.444	0.525	593.8	896.95	1.848	170.706
170.857	0.301	1108	1224.78	1.354	171.007
171.092	0.171	1826	1533.09	1.081	171.178
173.073	3.791	57.04	1651.43		174.968
		FUSION RUNS G			
159.672	21.148	46.78	625.38	2.651	170.247
170.684	0.872	980.3	1464.71	1.132	171.119
173.349	4.460	68.47	1655.18		175.579
Melting Point: This sample				(1.000)	171.132
Melting Point: Pure compound				(0.000)	172.008

Figure 17

Fractional Fusion Curve for Perchloric Acid

Legend:

○ Fusion Runs B

□ Fusion Runs G

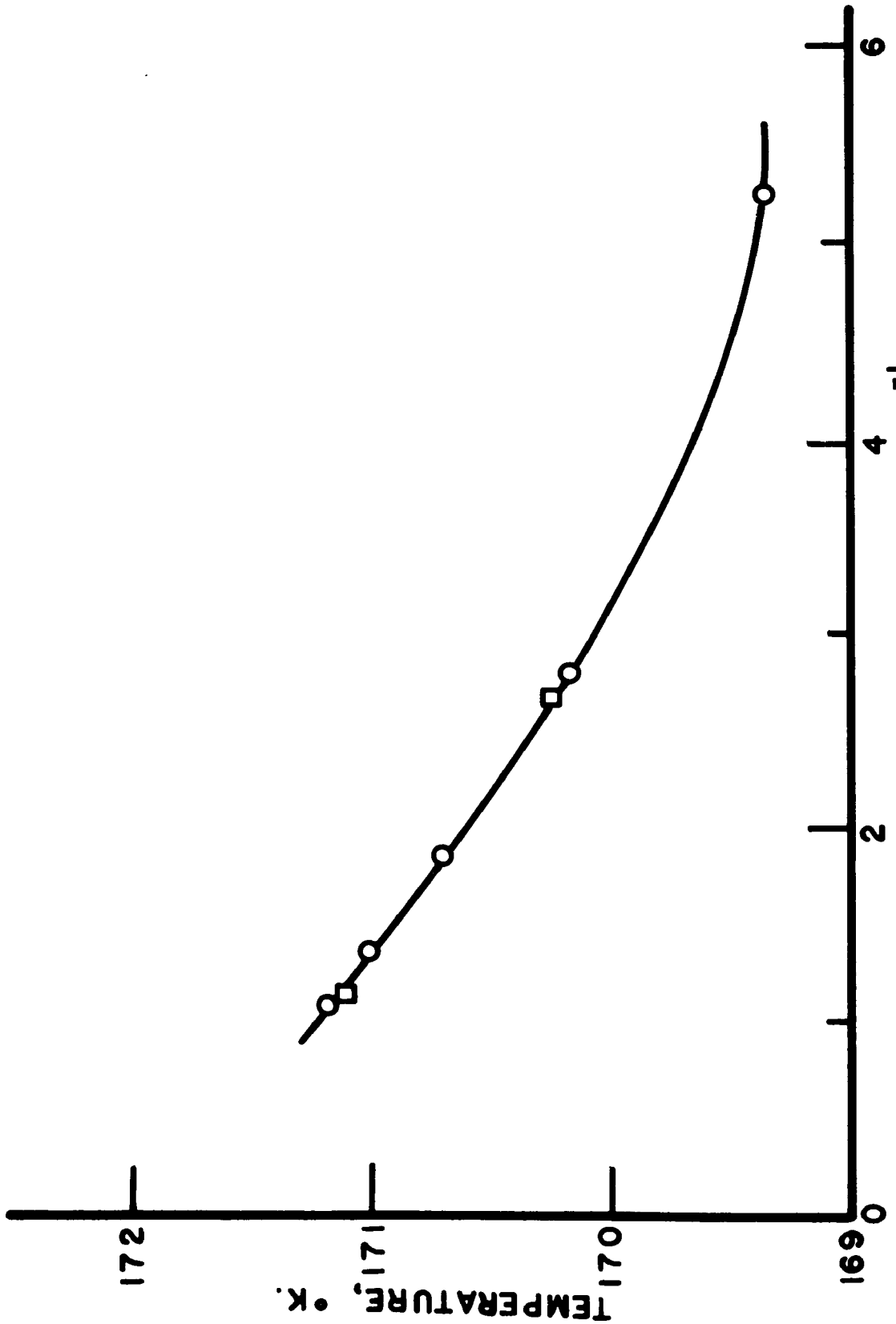


Figure 17

TABLE XII

THERMODYNAMIC FUNCTIONS OF PERCHLORIC ACID

($HClO_4$; 1 mole 100.465g.; Units: cal., mole, °K.)

T	C_p	S°	$H^\circ-H_0^\circ$	$-(F^\circ-H_0^\circ)/T$
		CRYSTAL		
5	0.034	0.011	0.042	0.003
10	0.300	0.088	0.672	0.021
15	1.005	0.330	3.770	0.079
20	2.037	0.755	11.28	0.191
25	3.204	1.334	24.36	0.359
30	4.369	2.021	43.30	0.578
35	5.449	2.777	67.90	0.838
40	6.389	3.568	97.55	1.129
45	7.199	4.369	131.57	1.445
50	7.907	5.164	169.37	1.777
60	9.125	6.717	254.70	2.472
70	10.18	8.205	351.36	3.185
80	11.11	9.627	457.96	3.902
90	11.91	10.983	573.16	4.614
100	12.60	12.273	695.73	5.316
110	13.26	13.505	825.00	6.005
120	13.95	14.688	960.99	6.680
130	14.70	15.834	1104.2	7.340
140	15.50	16.952	1255.2	7.987
150	16.36	18.050	1414.4	8.621
160	(17.33)	19.137	1582.8	9.244
171.13	(18.25)	20.323	1779.0	9.919
		LIQUID		
171.13	(26.06)	29.999	3436.0	9.919
180	26.14	31.302	3664.7	10.942
190	26.25	32.718	3926.6	12.052
200	26.43	34.069	4190.0	13.119
210	26.62	35.364	4455.3	14.148
220	26.83	36.607	4722.5	15.141
230	27.04	37.804	4991.8	16.100
240	27.26	38.959	5263.3	17.029
250	27.49	40.077	5537.1	17.928

TABLE XII (Cont.)

260	27.73	41.160	5813.2	18.801
270	27.98	42.210	6091.7	19.649
280	28.25	43.233	6372.9	20.472
290	28.55	44.229	6656.9	21.274
300	28.75	45.198	6943.8	22.059
273.15	28.07	42.535	6180.0	19.910
298.15	28.80	45.024	6890.9	21.911

TABLE XIII

ENTHALPY AND ENTROPY INCREMENTS OF PERCHLORIC ACID

(Units: cal., mole, ^{o}K.)

Designation	Energy Increments	T_{final}	$T_{initail}$	$H^{o}_{180}-H^{o}_{150}$	$S^{o}_{180}-S^{o}_{150}$
		FUSION			
Series VI*	12	180.05	150.26	(2244.8)	(13.218)
Series VII	2	181.63	150.00	2250.6	13.252
Series VIII	2	181.61	151.72	2251.4	13.255
Series XI	4	179.96	149.10	2248.5	13.245
RUN A**	1	183.55	147.21	(2258.8)	(13.300)
RUN F	1	175.04	148.57	2250.8	13.252
RUN H	1	183.20	149.71	2250.4	13.251
		Average		2250.3	13.251
		CRYSTAL		$H^{o}_{150}-H^{o}_{110}$	
Series VI	5	150.26	112.30	589.69	
Series XII	5	152.24	108.85	588.96	
RUN D	1	151.72	110.67	588.16	
		Average		589.27	
Numerical Quadrature of Smoothed Curve:				589.42	

* Rejected from average due to long time (4.5 days) necessary to attain desired drift.

** Rejected from average by Chauvenet's criterion.

DISCUSSION

Triethylenediamine

Triethylenediamine, a nearly spherical molecule (a homolog of bicyclo [2,2,2] octane) has been investigated at room temperature (crystal II) by X-ray analysis according to Wada, et al. [33] who also did qualitative differential thermal studies on the transition first reported by Farkas, et al.[34] and fusion. These data, combined with the information obtained from this research, are still not definitive enough to account for the magnitude of the entropy increment of the solid-solid transition. According to Guthrie and McCullough molecular orientations that are energetically favorable usually will be among those for which the approximate symmetry elements of the molecule are aligned with the symmetry elements of the lattice. Thus, for favorable orientations the effective point symmetry of the molecule will be a sub-point group of the crystal symmetry at the lattice site, and the number of possible distinguishable orientations can be estimated from symmetry considerations. Using this theory an entropy term of only R ln 8 (4.13 cal. $mole^{-1}$ $^{o}K.^{-1}$) would be allowed for triethylenediamine whereas a value of 7.19 cal. $mole^{-1}$ $^{o}K.^{-1}$ was found experimentally. The calculated value would arise from assuming a molecular symmetry of D_{3h} and finding the most likely distinguishable orientations of the molecule at an O_h lattice site. With this assignment the 3-fold molecular axis could be aligned with each of the four

3-fold axes of the cubic lattice in two different ways differing by a 60° rotation about the molecular axis.

It has been reported by Hendrickson[35] that in the case of bicyclo[2,2,2] octane the molecule would be most favorably arranged in a twisted conformation allowing the hydrogens on the ethylene groups to be situated at positions where the potential energy is at a minimum rather than at a maximum as in a D_{3h} configuration. This twisting reduces the molecular symmetry to D_3 which leads to several interesting ramifications.

Wada, et al. reported the space group of the crystal II phase to be C_{6h}^2. If this is assumed to be true, it is not possible for the molecule to be twisted in this temperature region, but twisting could take place at the transition temperature leading to a transition increment of R ln 16 (5.51 cal. $mole^{-1}$ $^oK.^{-1}$) since both a right-handed and left-handed twist would be equally probable. However, X-ray analysis is seldom able to distinguish conclusively between C_{6h}^2 and C_6^6 which is the space group for D_3 molecular symmetry in this case.

If the true molecular symmetry is D_3 at room temperature, a right-handed and left-handed twist are still possible. By analogy to bicyclo [2,2,2] octane, triethylenediamine should therefore be twisted only a few degrees causing little crystal strain , and, since no thermal anomalies have been observed below room temperature,[27] it is possible that a residual entropy may exist at extremely low temperatures in the amount R ln 2. An entropy calculation from spectroscopic

data should point out any existing ambiguity.

The entropy values reported by Wada, et al. for the crystal II→I transition and fusion are not in agreement with those of this research. He reported the increments to be 6.62 cal. mole^{-1} °K.$^{-1}$ at 353.0°K. and 3.3 cal. mole^{-1} °K.$^{-1}$ at 434.3°K. respectively, while the corresponding increments from this study are 7.19 cal. mole^{-1} °K.$^{-1}$ at 351.09°K. and 4.10 cal. mole^{-1} °K.$^{-1}$ at 432.98 respectively. Not even purity considerations can reasonably account for the discrepancy.

It is interesting to note entropies of transition of two other bicyclo systems. Bicyclo [2,2,1] heptane[6] and 3-azabicyclo [3,2,2] nonane[36] have been studied thermally yielding transitional entropies of 7.53 cal. mole^{-1} °K.$^{-1}$ at 131.7°K. and 11.63 cal. mole^{-1} °K.$^{-1}$ at 297.78°K. respectively. Both compounds should have identical C_{2v} molecular symmetry and are presumed to be in the plastic crystalline region above their transitions. Therefore, symmetry considerations alone will not account for the magnitudes of the anomalies. Work is presently underway in this laboratory to investigate the fusion thermal effects of 3-azabicyclo [3,2,2] nonane to provide some insight into the mechanism of the solid state transition. More studies by X-ray diffraction and infra-red and Raman spectroscopy of crystals I and II would obviously be desirable.

Pentaerythrityl Fluoride

Taking into account only the change in symmetry features

on traversing the solid II→I transition (Figure 14) in pentaerythrityl fluoride, $C(CH_2F)_4$, Payne[30] could account for the magnitude and mechanism of the reaction. This mechanism was then applied to the solid phase anomaly in pentaerythritol, $C(CH_2OH)_4$, studied by Nitta[29] and found to predict exactly the experimental results after correction terms were added for the additional symmetry modes available to the hydrogen atoms.

Since the fusion properties of pentaerythrityl fluoride have been experimentally determined, a check is now possible on the effects of the hydrogen atoms in pentaerythritol. Because of the proximity in size of oxygen and fluorine atoms, the basic lattice heat capacity should be the same in both cases with differences in entropies due only to symmetry factors. Payne showed that this difference in configurational entropy would be $R \ln 2 + 4 R \ln 3 = 10.11$ cal. mole^{-1} °K.$^{-1}$. The entropies of transition and fusion in pentaerythritol are, respectively, 22.8 and 3.2 cal. mole^{-1}°K.$^{-1}$, while the corresponding increments are 12.66 and 3.35 cal. mole^{-1} °K.$^{-1}$ respectively for pentaerythrityl fluoride. A sum of the two transitions in each of these substances gives the disorder present above their common lattice energy. Subtracting this sum for the fluoride from that of the alcohol gives 26.0 - 16.0 = 10.0 cal. mole^{-1} °K.$^{-1}$. This is well within experimental error of the 10.1 cal. mole^{-1} °K.$^{-1}$ calculated by Payne and, as such, is further evidence for the proper choice of a mechanism for the observed transitions.

Perchloric Acid

The earliest reported melting temperature for perchloric acid was by Van Wyk[19] who used a pentane thermometer calibrated with a toluene thermometer from 0 to -70°C. His lower temperatures were obtained by extrapolation giving him a temperature of -112°C. (161°K.) for the melting point. From this research the true melting point of perchloric acid was taken as 172.01°K. Hence, the discrepancy suggests either that Van Wyk's calibration was seriously in error or that his mole fraction of impurity (possibly perchloric acid monohydrate) was significantly greater than for the present sample.

Zinov'ev and Rosolovskii[22] presented an incomplete phase diagram for the system chlorine heptoxide (Cl_2O_7)-water from 25 to 100 mole percent chlorine heptoxide. A copy of the relevant portion of their diagram appears in Figure 18. They report a eutectic at 53 mole percent chlorine heptoxide and 173 $\pm$ 2°K. and state in contradiction to their phase diagram that this is the melting point of perchloric acid ($HClO_4$) but also mention that there is no "crystallization line" for this substance. As presented, their data show neither a maximum (congruent melting point) nor a peritectic melting at or near the region of 50 mole percent chlorine heptoxide corresponding to perchloric acid and imply that this substance disproportionates in the solid phase to a mixture of perchloric acid monohydrate and chlorine heptoxide.

Assuming the phase diagram of Zinov'ev and Rosolovskii

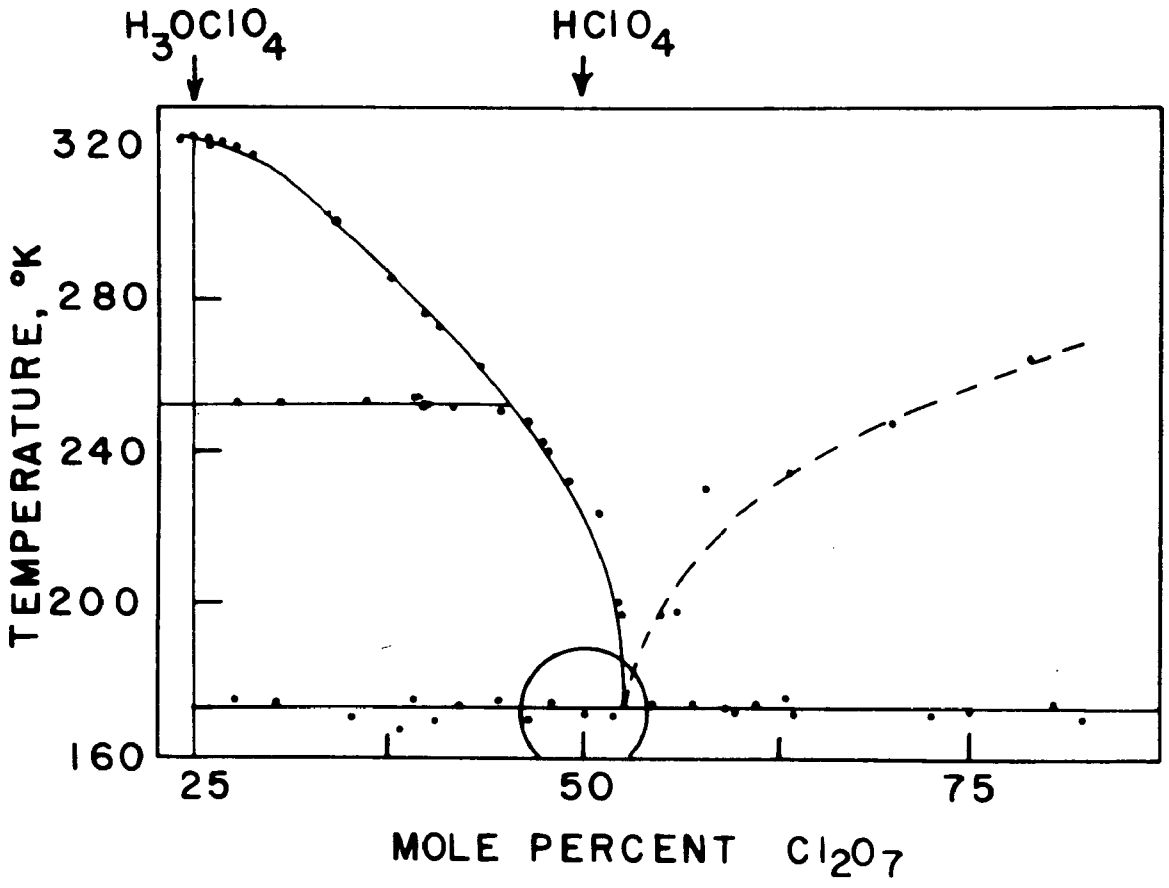
Figure 18

Phase Diagram of the System Chlorine Heptoxide-Water

Legend:

Upper - From Zinov'ev and Rosolovskii[22]

Lower - Hypothetical congruent melting maximum at molecular perchloric acid


H_3OClO_4
$HClO_4$
320
280
240
200
160
TEMPERATURE, °K
25
50
75
MOLE PERCENT Cl_2O_7

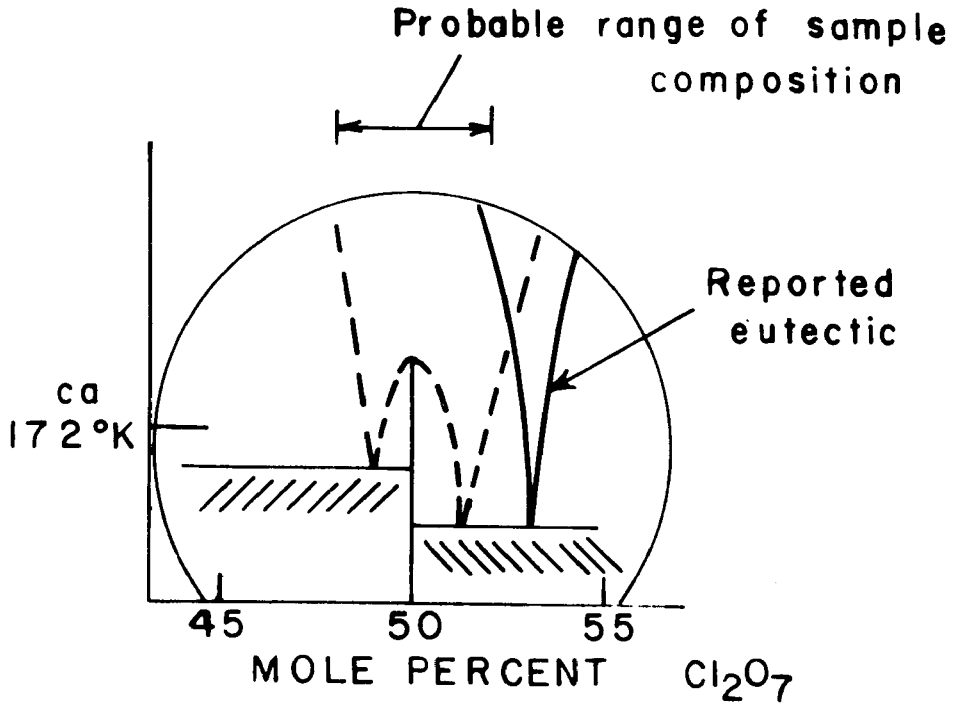

Probable range of sample composition
Reported eutectic
ca 172°K
45
50
55
MOLE PERCENT Cl_2O_7

Figure 18

to be correct, the thermal anomaly observed by this calorimetric research corresponds to the situation at the eutectic composition rather than to that indicated as 50 mole percent on their daigram. For, were the latter situation correct, a second thermal effect would have been obtained over the entire region from 173 ± 2°K. terminating in the complete melting of the sample at 222°K. The following considerations permit an estimate of the magnitude of this (undetected) effect. If the calorimetric sample did correspond to the composition 50 mole percent on the phase diagram, about 90% of the total thermal effect would be expected to appear at the eutectic temperature (from the length of the tie lines) and the remaining 10% should appear over the region 173-222°K. with some concentration in the upper part of the range if the melting curve slope is reliable. However, since the observed heat capacities at all temperatures above the eutectic appear to be nearly linear and certainly not 4 cal. $mole^{-1}$ $°K.^{-1}$ higher than normal over the range 173-222°K., the phase diagram reported may be assumed to be in error in one of two ways. Either (1) the analyses of the samples used in the phase study are wrong shifting the limit of saturation curve such that the eutectic is almost exactly at 50 mole percent chlorine heptoxide, (2) "fine structure" in the vicinity of 50 mole percent of the diagram (circled portion in Figure 18) was not detected, or both.

The titrimetric method used by Zinov'ev and Rosolovskii

yields results in weight percent after weighing, separation, dilution and titration. In the conversion from weight to mole percent an error of about 0.5% in the former would lead to 3% error for the latter in the concentration range near 50 mole percent chlorine heptoxide. In view of this fact and the difficulty in an analysis of perchloric acid at high acid concentrations, it is not unlikely that the eutectic composition is sufficiently in error to place it at 50 mole percent.

The second type of error above is purely hypothetical yet not inconsistent with experimental fact. The presence of a congruent melting point for perchloric acid would suggest its stability (and lack of disproportionation) in the solid. The circled portion of the phase diagram in Figure 18 is enlarged at the bottom of the figure showing a hypothetical congruent fusion in the saturation curve allowing solid perchloric acid to form. The shaded areas of the figure point out that neither eutectic region has been sharply defined experimentally except for the existence of a transition in this region. The two eutectic temperatures, however, might differ by less than a degree. The peak height is estimated to be about two degrees or less since the eutectic temperature reported by Zinov'ev and Rosolovskii is close to the fusion temperature measured by this research. The exact purity of the perchloric acid sample studied calorimetrically is still in doubt as indicated in Figure 18. The rise in heat capacity prior to fusion is probably a combination of impurity premelting and the exothermic eutectic

transition.

A recent Raman spectroscopic study by Taylor and Dahl[39] of solid perchloric acid is shown schematically in Figure 19. The sample investigated was withdrawn at the same time the calorimeter was loaded for this cryogenic research, stored in liquid nitrogen, and the spectrum taken with the sample submerged in liquid nitrogen. The following frequencies were observed (in $cm.^{-1}$): 463 ± 8, 585 ± 2, 738 ± 2, 1038 ± 2, 1243 ± 2, 1550 ± 3, 2329 ± 2, 2602 ± 2, 3040 ± 5, 3336 ± 5. The line at 2329 $cm.^{-1}$ is due to nitrogen while the line at 2602 $cm.^{-1}$ is from the mercury source. Agreement between this sample and that of liquid perchloric acid is satisfactory to prove the existence of this compound in the solid state. A comparison of the other spectra of Figure 19 shows that the perchlorate ion, perchloric acid monohydrate and chlorine heptoxide are not present in measurable amounts. The two significant lines at about 925 $cm.^{-1}$ and 1115 $cm.^{-1}$ in the perchlorate ion spectra are missing from the solid acid spectra as is the line at 501 $cm.^{-1}$ in chlorine heptoxide and the very intense line at 921 $cm.^{-1}$ for the monohydrate. This spectral evidence, therefore, confirms the existence of the species $HClO_4$ in the solid phase and supports the possible correctness of the general behavior proposed in the lower portion of Figure 18 in the chlorine heptoxide-water phase diagram.

The sample of perchloric acid used for calorimetric investigation was subjected to several tests after the low temperature measurements. Conductometric titrations were carried

Figure 19

Schematic Comparison of Raman Spectra

Legend:

A. $HClO_4$ (l), Simon and Weist[10]

B. $HClO_4$ (l), Fonteyne[37]

C. $HClO_4$ (l), Landolt - Bornstein[38]

D. $HClO_4$ (s), Taylor and Dahl[39]

E. ClO_4^-, Simon and Weist[10]

G. H_3OClO_4, (s) Taylor and Vidale[16]

H. Cl_2O_7, Fonteyne[40]

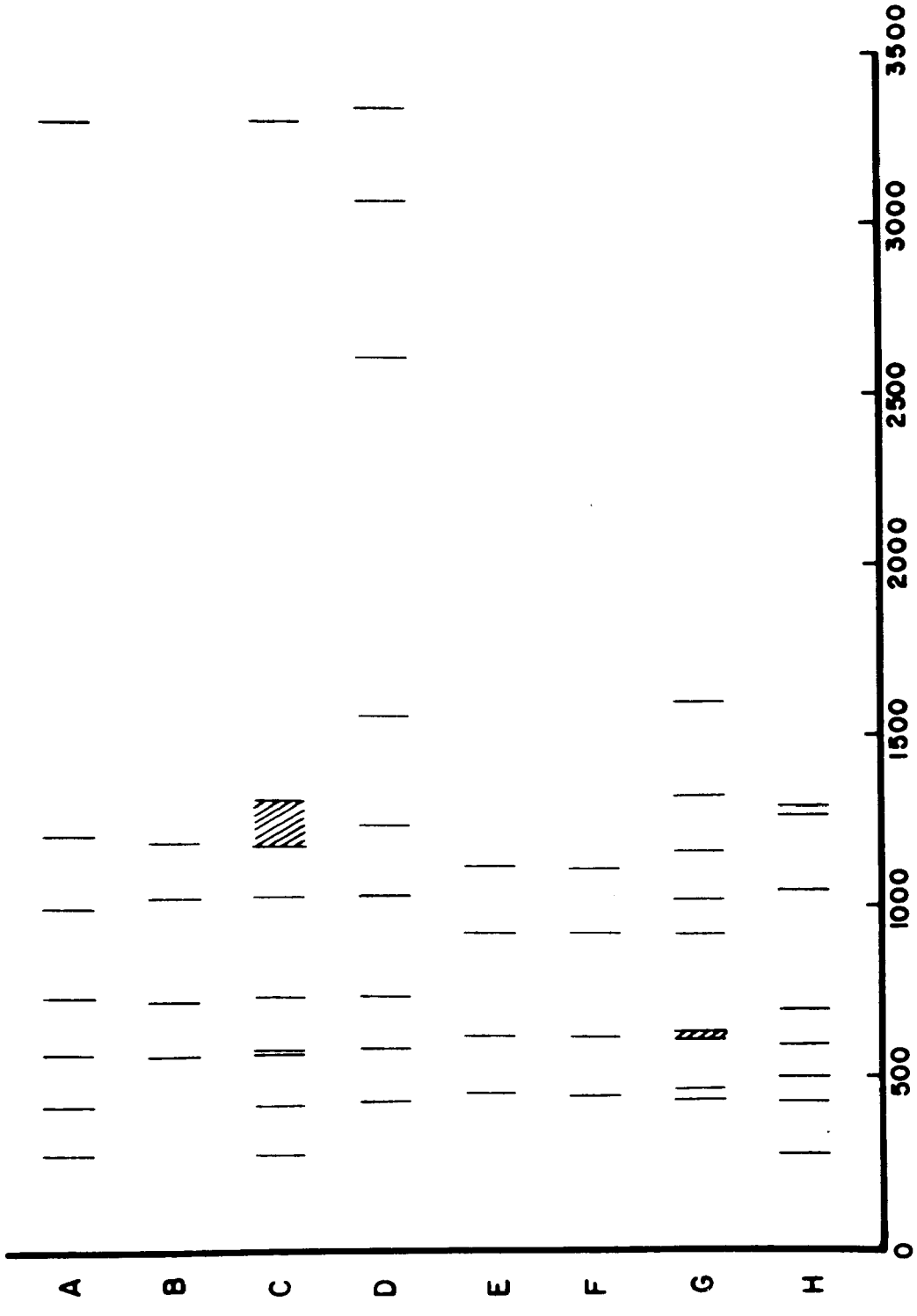


Figure 19

out for both the acid and perchlorate content. The results showed about 5% impurity (by weight) for both species and substantiated visual evidence that the sample had decomposed prior to removal from the calorimeter and was still spontaneously decomposing. A strong, yellow color was present when the sample was unloaded and over a period of about six hours turned to dark orange on standing at room temperature. The color is most probably due to the presence of ozone as mentioned by Smith[41] or of chlorine which is claimed to be a decomposition product of perchloric acid by Zinov'ev and Tsentsiper.[12] Several attempts were made to identify the contaminant by infra-red spectroscopy, but the impurity was too dilute to permit detection in a liquid sample and too soluble to permit separation as a gas.

From spectroscopic studies of Giguere and Savoie[42] the entropy of gaseous perchloric acid at 298°K. in the ideal gas state was reported as 70.7 cal. mole^{-1} °K.$^{-1}$. A recent communication from Professor P.A. Giguere[43] indicates that this should be corrected to 70.5 cal. mole^{-1} °K.$^{-1}$. Since only very scattered vapor pressure measurements were available from the literature some doubt is entertained as to the validity of including a calculation of the entropy of vaporization from the liquid to the ideal gas state. However, using the two single vapor pressure measurements (18 mm. at 16°C. [19] and 56 mm. at 39°C. [44]) of questionable reliability available from different sources and using the Clausius-Clapeyron equation and ideal gas behavior, entropy terms of 29.7

cal. mole^{-1} ^{o}K.$^{-1}$ for vaporization and -6.5 cal. mole^{-1} ^{o}K.$^{-1}$ for compression should be added to the entropy of liquid perchloric acid at 298.15^{o}K. yielding an ideal gas value of 68.2 ± 1.9 cal. mole^{-1} ^{o}K.$^{-1}$ at that temperature and one atmosphere pressure (see Table XIV). Since the agreement with spectroscopic data is probably within experimental error of the estimated entropy of vaporization there is no reason to suspect residual entropy on the basis of the present measurements. It is perhaps more meaningful to estimate the entropy of vaporization from the difference between the two measured entropies. At 298.15^{o}K. the calculated value would be 32.0 cal. mole^{-1} ^{o}K.$^{-1}$ which corresponds to an enthalpy increment of 9.55 kcal. mole^{-1} assuming the perchloric acid vapor behaves as an ideal gas.

An estimate of the effect of the apparently impure nature of the sample (2.5 mole percent) studied by this research on the thermodynamic functions can be made allowing the following assumptions: (1) the impurity is only perchloric acid monohydrate and (2) the ideal additivity of the heat capacities of water and perchloric acid. With these in mind, it was calculated that the enthalpy, entropy, and free energy functions may be in excess by maximum values of approximately 46 cal. mole^{-1}, 0.20 cal. mole^{-1} ^{o}K.$^{-1}$ and 0.05 cal. mole^{-1} ^{o}K.$^{-1}$ at 298.15 ^{o}K., respectively.

TABLE XIV

ENTROPY OF GASEOUS PERCHLORIC ACID AT 298.15 °K.

(Units: cal., mole, °K.)

0-5 °K. Debye extrapolation	0.011
5-171.13 °K., solid, numerical integration	20.312
Fusion, 1657.0/171.13	9.676
171.13-298.15 °K., liquid, numerical integration	15.025
Vaporization at 28.7 mm., 8852/298.15	29.690
Compression from 28.7 mm. to 760 mm, -R ln(760/28.7)	-6.511
Total, $S^{o}_{298.15}$ (Gas, 1 atm.)	68.20
Spectroscopic,[43] $S^{o}_{298.15}$ (Gas, 1 atm.)	70.5

APPENDIX I

Digital Computer Program for Vaporization and Sublimation Correction

In the course of this research it became necessary to make several corrections for the heats involved in vaporizing or subliming part of the sample while making heat capacity measurements. For these corrections use was made of the IBM 709 digital computer and the Michigan Algorithm Decoder (MAD) computer language. The version of the correction program that appears here has been in effect since July 31, 1962.

In this program, the basic logic is patterned after that used by Hoge[45] and is shown in Figure A. Table A gives the input card formats used in the computation. The program will correct only one compound at any time, but that compound may be divided into any number of regions such that data for all solid phases and the liquid phase may be corrected in one loading of the computer. To correct the second and following sections the Calorimeter and Sample Constants Card is not included since the computer will use the information given by the first section.

The program was written to be as general as possible in several features. The vapor pressure equation can be run with any of its constants as zero allowing basically different equations to be used. A correction is incorporated to allow for the gas phase volume increase due to vaporization

Figure A

Logic for Sublimation and Vaporization Correction

Legend:



= Have all data points been read?



= Have the properties at the initial and final temperatures been calculated?



= Have the desired number of iterations been completed?

$P = f(T) = 10^{(X + Y/T + Z \log T)}$

$V = f(W,P) = V_c - W/(\rho - d\rho/dT \times (T-T_\rho))$

$W = f(P,V,T) = W' - PxVxM/(RxT + bxP)$

$n = f(W) = PxV/(RxT+bxP)$

Q_s = Corrected energy (cal.)

Q = Total energy (cal.)

Q_g = Energy absorbed by gas phase (cal.)

Q_{trans} = Energy absorbed upon sublimation or vaporization (cal.)

P = Partial pressure of sample (mm, atm., etc.)

X, Y, and Z = Constants in vapor pressure equation

T = Temperature ($^oK.$)

V = Volume available to gas phase (cc.)

V_c = Internal volume of empty calorimeter (cc.)

W and W' = Weight of sample (g.)

ρ = Density of sample at a temperature, T (g. $cc.^{-1}$)

$d\rho/dT$ = Change in density with temperature (g. $cc.^{-1}$ $^oK.^{-1}$)

M = Molecular weight of sample (g.)

R = Gas constant (mm. cc. $mole^{-1}$ $^oK.^{-1}$, atm. cc. $mole^{-1}$ $^oK.^{-1}$, etc.)*

b = Van der Waal's constant (cc. $mole^{-1}$)

n = Number of moles of sample in gas phase

* Units to be a self consistent set.

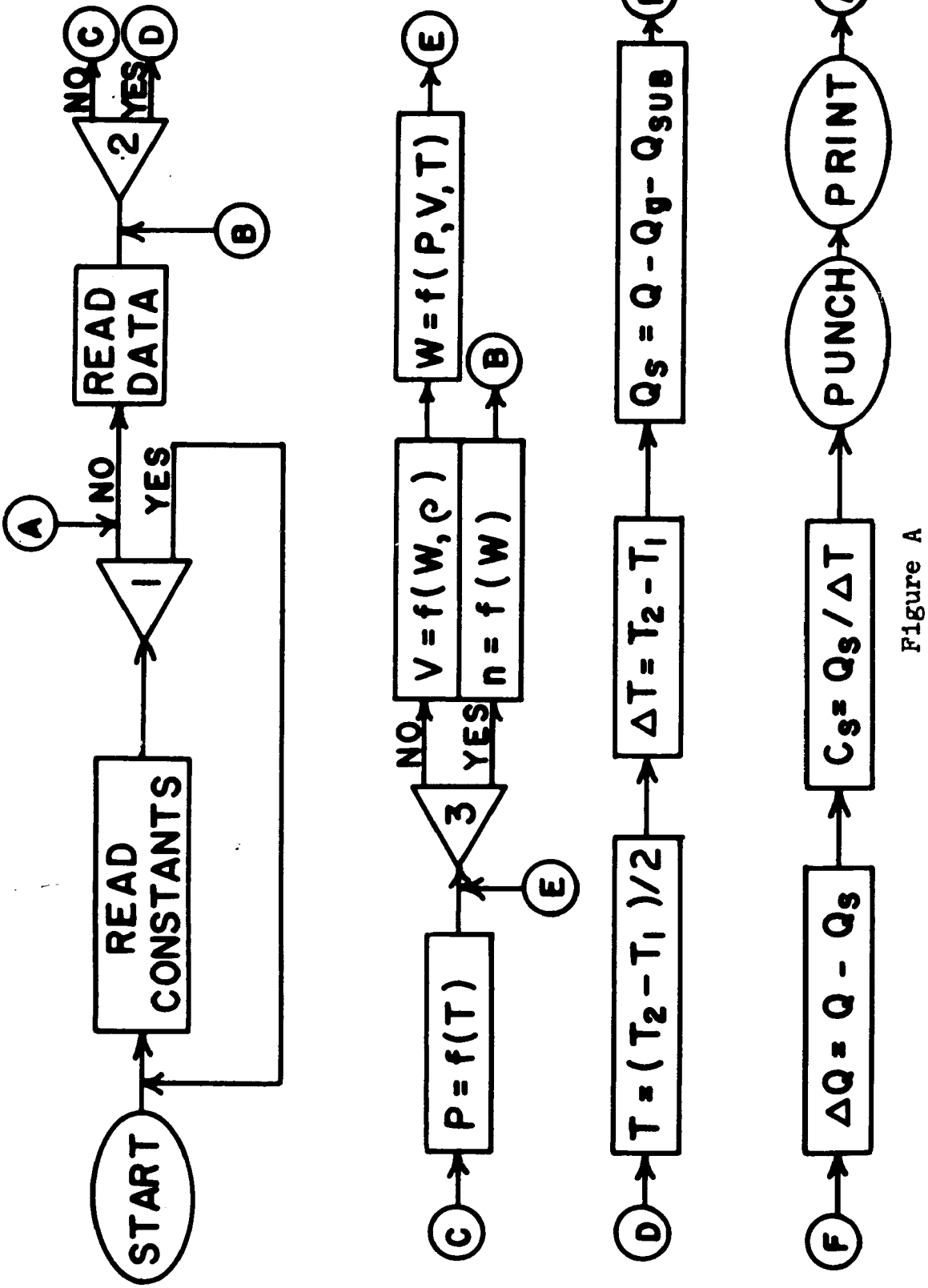

START
READ CONSTANTS
1
NO
YES
A
READ DATA
2
NO
YES
C
D
B
P = f(T)
C
3
NO
YES
E
V = f(W,)
n = f(W)
W = f(P,V,T)
E
B
T = (T2 - T1)/2
D
ΔT = T2 - T1
Qs = Q - Qg - QSUB
F
ΔQ = Q - Qs
F
Cs = Qs / ΔT
PUNCH
PRINT
A

Figure A

TABLE A

CARD FORMATS FOR VAPORIZATION AND SUBLIMATION CORRECTION

COLUMNS	FUNCTION	DIGITS*
	Calorimeter and Sample Constants Card	
1 - 10	Volume of empty calorimeter	xxxx,xxxxxx
11 - 20	Molecular weight of sample	xxxx,xxxxxx
21 - 30	Mass of sample (in vacuo)	xxxx,xxxxxx
31 - 43	Gas constant, R	.xxxxxxxxE ± xx
44 - 56	Van der Waal's constant, b	.xxxxxxxxE ± xx
57 - 58	Number of iterations desired	xx
	Hollerith Card	
1 - 80	Title of calculation, date, etc.	
	Vapor Pressure and Density Card	
1 - 3	Number of data points	xxx
4 - 14	X }	xxxxx,xxxxxx
15 - 25	Y } In log $P = X + Y/T + Z \log T$	xxxxx,xxxxxx
26 - 36	Z }	xxxxx,xxxxxx
37 - 49	Density of sample at T_d	.xxxxxxxxE ± xx
50 - 62	Temperature, T_d	.xxxxxxxxE ± xx
63 - 75	Change of density with temp.	.xxxxxxxxE ± xx
	Enthalpy Card	
1 - 10	Temperature at which ΔH_{trans} was measured, T_o	xxxx,xxxxxx
11 - 23	ΔH_{trans} at T_o	.xxxxxxxxE ± xx
24 - 36	A }	.xxxxxxxxE ± xx
37 - 49	B } in $C_{p(g)} = A + BT$	.xxxxxxxxE ± xx
50 - 62	C }	.xxxxxxxxE ± xx
63 - 75	D } in $\Delta H_t = \Delta H_{t_o} + (C + DxT)(T - T_o)$	.xxxxxxxxE ± xx

TABLE A (Cont.)

Apparent Heat Capacity - Temperature Data Card

1 - 3	Run number	xx
4 - 16	Energy of run	.xxxxxxxxE ± xx
17 - 29	T_1 (Lower temperature)	.xxxxxxxxE ± xx
30 - 42	T_2 (Upper temperature)	.xxxxxxxxE ± xx

* Note: Commas which appear in fixed point numbers represent decimal points that do not need to be punched. All listed decimal points should be punched in their respective floating point fields. Fields listed without commas or decimal points are integer fields and leading zeros must be punched.

or sublimation of the sample and to adjust the volume of the solid or liquid for the change in volume with temperature. Also included are corrections to allow for the heat of sublimation or vaporization as a function of temperature and to correct for the heat capacity of the sample in the gas phase.

It is evident that not all desired data may be available, but approximations may be used or a zero value run in lieu of data in most cases. For $d\rho/dT$ a usable value for solids is often 1×10^{-5} g. cc.$^{-1}$ ^{o}K.$^{-1}$ while the Van der Waal's constant, b, is approximated as four times the volume of one mole of molecules. Inclusion of the constant, b, in the gas equation of state often makes an appreciable difference and should be used whenever possible.

The Apparent Heat Capacity-Temperature Data Cards are the output from the run calculation[46] and can be corrected in any order. The punched output is the same format as the input and can be used directly in further calculations. The printed output lists in left to right order the quantities ΔQ, Q, T_1, T_2, ΔT, T, and C_s which have been previously defined.

BIBLIOGRAPHY

1. E.F. Westrum, Jr., J. Chem. Ed. 30, 443 (1962).
2. J. Timmermans, J. chem. phys. 35, 331 (1938).
3. J. Timmermans, Ind. chem. belge 16, 178 (1951).
4. E.R. Andrew, J. Chem. Phys. 18, 607 (1950).
5. W.L. Dunning, J. Phys. Chem. Solids 18, 21 (1961)
6. G.B. Guthrie and J.P. McCullough, J. Phys. Chem. Solids 18, 53 (1961).
7. L.A.K. Staveley, Ann. Rev. Phys. Chem. 13, 351 (1962).
8. F. von Stadion, Ann. chim. et phys. 8, 406 (1818).
9. Joseph C. Schumacher, Ed., "Perchlorates: Their Properties, Manufacture and Uses", p. 11, Reinhold, New York (1960).
10. A. Simon and M. Weist, Z. anorg. u. allgem. Chem. 268, 301 (1952).
11. A.E. Missan and A.M. Sukhotin, Zhur. Neorg. Khim. 4, 606 (1959).
12. A.A. Zinov'ev and A.B. Tsentsiper, Russian J. Inorg. Chem. 4, 329 (1959).
13. G.F. Smith, J. Am. Chem. Soc. 75, 184 (1953).
14. M. Usanovich and T. Sumarokiva, Acta Physicochim. U.R.S.S. 21, 836 (1946).
15. O. Redlich, E.K. Holt and J. Bigeleisen, J. Am. Chem. Soc. 66, 13 (1944).
16. R.C. Taylor and G.L. Vidale, J. Am. Chem. Soc. 79, 5599 (1956).
17. M. Usanovich, T. Summarokova and V. Udovenko, Acta Physicochim. U.R.S.S. 11, 505 (1939).
18. M. Berthelot, Ann. chim. phys. 27, 214 (1882).
19. H.J. Van Wyk, Z. anorg, Chem. 48, 1 (1906).
20. L.H. Brickwedde, J. Research Natl. Bur. Standards 42, 309 (1949).

21. C.F. Goodeve and A.E.L. Marsh, J. Chem. Soc. 1937, 1816 (1937).

22. A.A. Zinov'ev and V. Ya. Rosoluskii, Zhur. Neorg. Khim. 3, 2382 (1958).

23. H.G. Carlson, "Thermodynamic Properties of Methyl Alcohol, 2-methyl-and 2,5-dimethylthiophene and 2-methyl furan", Doctoral Dissertation, to be published by University Microfilms.

24. E.F. Westrum, Jr., J.B. Hatcher and D.W. Osborne, J. Chem. Phys. 21, 419 (1953).

25. G.T. Furukawa, T.B. Douglas, R.E. McCoskey and D.C. Ginnings, J. Research Natl. Bur. Standards 57, 67 (1956).

26. E.D. West and D.C. Ginnings, J. Research Natl. Bur. Standards 60, 309 (1958).

27. S.S. Chang and E.F. Westrum, Jr., J. Phys. Chem. 64, 1551 (1960).

28. D.D. Tunnicliff and H. Stone, Anal. Chem. 27, 73 (1955).

29. I. Nitta, T. Watanabe, S. Seki and M. Momotani, Proc. Japan Acad. 26, 10 19 (1950).

30. D.H. Payne, "Low Temperature Thermodynamic Studies of Pentaerythritol and its Halide Derivatives", Doctoral Dissertation, University Microfilms Publication Number 11,336 (1954).

31. S.V.R. Mastrangelo and R.W. Dornte, J. Am. Chem. Soc. 77, 6200 (1955).

32. A.A. Zinov'ev, Ahur: Neorg. Khim. 3, 1205 (1958).

33. T. Wada, E. Kishida, Y. Tomiie, H. Suga, S. Seki and I. Nitta, Bull. Chem. Soc. Japan 33, 1317 (1960).

34. A. Farkas, G.A. Mills, W.E. Erner and J.B. Maeker, J. Chem. Eng. Data 4, 334 (1959).

35. J.B. Hendrickson, Chem. and Eng. News 39, 47, 40 (1961).

36. E.F. Westrum, Jr., unpublished data.

37. R. Fanteyne, Nature 138, 886 (1936).

38. Landolt - Bornstein, I. Band, Atom - and Molekularphysik, 2. Teil, Molekeln I, p551 (1951).

39. R.C.Taylor and A.J. Dahl, unpublished data.

40. R. Fonteyne, Natuurw Tijdschr. 21, 141 (1939).

41. G.F. Smith, private communication.

42. P.A. Giguere and R. Savoie, Canadian J. Chem. 40, 495 (1962).

43. P.A. Giguere, private communication.

44. D. Vorlander and R. von Schilling. Liebig's Ann. 310, 369 (1900).

45. H.J. Hoge, J. Research Natl. Bur. Standards 36, 111 (1946).

46. B.H. Justice, "Thermodynamic Properties and Electronic Energy Levels of Eight Rare Earth Sesquioxides", Doctoral Dissertation, University Microfilms Publication Number 63,376 (1961).